

# OpenScan: A Benchmark for Generalized Open-Vocabulary 3D Scene Understanding

Youjun Zhao<sup>1</sup>, Jiaying Lin<sup>1,2,\*</sup>, Shuquan Ye<sup>1,3</sup>, Qianshi Pang<sup>4</sup>, Rynson W.H. Lau<sup>1,\*</sup>

<sup>1</sup> City University of Hong Kong

<sup>2</sup> The Hong Kong University of Science and Technology

<sup>3</sup> The Chinese University of Hong Kong <sup>4</sup> South China University of Technology

## Abstract

Open-vocabulary 3D scene understanding (OV-3D) aims to localize and classify novel objects beyond the closed set of object classes. However, existing approaches and benchmarks primarily focus on the open vocabulary problem within the context of object classes, which is insufficient in providing a holistic evaluation to what extent a model understands the 3D scene. In this paper, we introduce a more challenging task called Generalized Open-Vocabulary 3D Scene Understanding (GOV-3D) to explore the open vocabulary problem beyond object classes. It encompasses an open and diverse set of generalized knowledge, expressed as linguistic queries of fine-grained and object-specific attributes. To this end, we contribute a new benchmark named *OpenScan*, which consists of 3D object attributes across eight representative linguistic aspects, including affordance, property, and material. We further evaluate state-of-the-art OV-3D methods on our OpenScan benchmark and discover that these methods struggle to comprehend the abstract vocabularies of the GOV-3D task, a challenge that cannot be addressed simply by scaling up object classes during training. We highlight the limitations of existing methodologies and explore promising directions to overcome the identified shortcomings.

**Code, Datasets, and Extended version —**

<https://youjunzhao.github.io/OpenScan/>

## Introduction

Open-vocabulary 3D scene understanding (OV-3D) involves recognizing object classes that are not included in the training set. It is important to applications like autonomous driving (Bojarski et al. 2016) and robotics (Zeng et al. 2018). Recently, vision-language models (VLMs), e.g., CLIP (Radford et al. 2021), have achieved significant progress by leveraging large-scale image-text datasets with semantically rich captions. The impressive capability of VLMs in capturing rich contexts between images and texts has inspired further exploration in open-vocabulary tasks in both 2D (Gu et al. 2022; Zhong et al. 2022) and 3D (Takmaz et al. 2023; Peng et al. 2023) domains.

For AI systems, the capability to comprehend diverse linguistic aspects of object-related attributes and their association with corresponding objects is as important as the iden-

\* Jiaying Lin and Rynson Lau are the corresponding authors.  
Copyright © 2026, Association for the Advancement of Artificial Intelligence (www.aaai.org). All rights reserved.

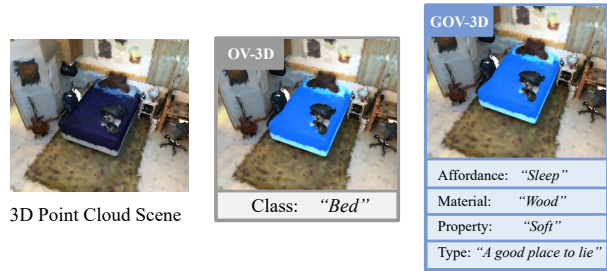


Figure 1: The proposed Generalized Open-Vocabulary 3D Scene Understanding (GOV-3D) task expands the vocabulary types of the classic 3D Scene Understanding (OV-3D) task. While OV-3D only supports queries of object classes, GOV-3D supports queries of object-related abstract attributes.

tification of the objects themselves. Consequently, the field of open-vocabulary 3D scene understanding should ideally extend beyond specific object classes to encompass complex object-related attributes, such as affordance and material, articulated through natural languages. However, the generalization ability of existing OV-3D methods (Peng et al. 2023; Takmaz et al. 2023; Yan et al. 2024; Yin et al. 2024; Nguyen et al. 2024) to object-related attributes has not been thoroughly and systematically explored. Besides, evaluating the ability of an OV-3D model to recognize specific object attributes is difficult due to the shortage of large-scale OV-3D attribute benchmarks. Existing OV-3D benchmarks, such as ScanNet (Dai et al. 2017) and ScanNet200 (Rozenberszki et al. 2022), primarily focus on object classes, and do not include annotations of object attributes for evaluating the generalized ability of OV-3D methods.

In this paper, we aim to study how well current OV-3D methods can generalize their understanding beyond 3D object classes to open-set object attribute vocabularies. Specifically, we introduce a more challenging task called Generalized Open-Vocabulary 3D Scene Understanding (GOV-3D). GOV-3D takes a 3D point cloud scene and a text query as input to predict a corresponding 3D mask of the best matching object, which is the same as OV-3D. However, unlike OV-3D which only supports object classes as the input text query, GOV-3D supports abstract vocabularies that specify the attribute of the target object in the input text query, as shown in Figure 1. This requires a comprehensive understanding of both 3D objects

and 3D scenes, making the GOV-3D task more challenging in practical scenarios.

Existing 3D scene understanding benchmarks, such as ScanNet (Dai et al. 2017), ScanNet200 (Rozenberszki et al. 2022), and ScanNet++ (Yeshwanth et al. 2023), only provide annotations for object classes. To address this limitation of existing benchmarks, we construct a new benchmark, named *OpenScan*, for the GOV-3D task. OpenScan is constructed based on the ScanNet200 (Rozenberszki et al. 2022) benchmark. It expands the single category of object classes in ScanNet200 into eight linguistic aspects of object-related attributes, including *affordance*, *property*, *type*, *manner*, *synonym*, *requirement*, *element*, and *material*. This allows each object to be associated with some generalized knowledge beyond object classes. With our OpenScan benchmark, it becomes possible to comprehensively evaluate existing OV-3D models from various aspects, enabling a quantitative assessment of their generalization capabilities in understanding abstract object attributes.

We have compared seven strong baseline methods under the GOV-3D task, on our OpenScan benchmark. Experimental results demonstrate that the current state-of-the-art OV-3D models excel in understanding basic object classes, but significantly degrade in their ability to understand object attributes, such as affordance and material. This highlights the importance of establishing a comprehensive and reliable benchmark to identify the weaknesses of OV-3D models. The key contributions of this work can be summarized as:

- We introduce a challenging task of Generalized Open-Vocabulary 3D Scene Understanding (GOV-3D) to extend the classic OV-3D task for a more general understanding of 3D scenes.
- We provide a novel benchmark named OpenScan for the GOV-3D task, which facilitates comprehensive evaluation of the generalization ability of OV-3D segmentation models on abstract object attributes.
- We conduct extensive experiments with existing OV-3D segmentation models on our OpenScan benchmark, showing that even the latest methods struggle to understand the abstract object attributes beyond object classes.

## Related Work

**Open-Vocabulary 3D Scene Understanding.** The study of open-vocabulary 3D scene understanding (Zhao, Lin, and Lau 2025) has been relatively limited compared to open-vocabulary 2D understanding. This is primarily due to the complexity and difficulty in obtaining 3D datasets. Open-Mask3D (Takmaz et al. 2023) introduces the open-vocabulary 3D instance segmentation task. It proposes the first approach for the task in a zero-shot setting. OpenScene (Peng et al. 2023) also proposes a zero-shot method for open-vocabulary 3D scene understanding. Beyond the object class, it is able to utilize arbitrary text queries for semantic segmentation. Previous methods have mainly focused on object context for 3D scene understanding. PLA (Ding et al. 2023) and RegionPLC (Yang et al. 2024) extend the context to a more coarse-to-fine semantic representation to provide a more comprehensive supervision. Recently, OpenIns3D (Huang et al.

2024), Open3DIS (Nguyen et al. 2024), and SAI3D (Yin et al. 2024) utilize powerful 2D segmentation models to generate 2D instances and then merge them into 3D instances. Instead of utilizing accurate 2D masks from 2D segmentation models, MaskClustering (Yan et al. 2024) leverages clustering algorithms to perform zero-shot 3D segmentation. Recently, UniSeg3D (Xu et al. 2024) proposes a unified framework for 3D scene understanding. However, these methods only provide qualitative results for object attributes and lack a thorough evaluation of performance beyond object classes. This motivates us to conduct a quantitative evaluation that encompasses a wider range of object attributes.

**3D Scene Understanding Benchmark.** Existing open-vocabulary 3D scene understanding benchmarks, *e.g.*, ScanNet (Dai et al. 2017), ScanNet200 (Rozenberszki et al. 2022), S3DIS (Armeni et al. 2016), and Matterport3D (Chang et al. 2017), utilize RGB-D cameras, while ARKitScenes (Baruch et al. 2021), Replica (Straub et al. 2019), and ScanNet++ (Yeshwanth et al. 2023) leverage high-resolution laser scanners to capture high-fidelity 3D data for 3D reconstructions. Our proposed OpenScan benchmark expands the object class annotations of the open-vocabulary 3D scene understanding benchmarks (*i.e.*, ScanNet200) to object-related attributes. Similar to the 3D referring (Chen, Chang, and Nießner 2020) and 3D reasoning (Huang et al. 2025) benchmarks, our OpenScan introduces new annotations for existing 3D scans to locate 3D objects via text queries. Unlike these tasks, which assume the queried object exists in the scene, our introduced GOV-3D task requires discriminative capabilities to determine whether the query presents in the scene. MMScan (Lyu et al. 2024) provides a benchmark for visual attribute understanding but lacks commonsense-related attribute annotations (*e.g.*, “*synonym*” and “*requirement*”) included in our OpenScan. Recently, SceneFun3D (Delitzas et al. 2024) provides a large-scale 3D dataset with annotations for functionality and affordance interactions in 3D scenes. However, our OpenScan differs from SceneFun3D by considering a broader range of attributes. Specifically, while SceneFun3D focuses on function or affordance understanding, our OpenScan covers eight linguistic aspects, with affordance representing just one of them. Besides, while SceneFun3D focuses on element-level human-scene interaction (*e.g.*, “*door handle*”), our OpenScan is designed for object-level scene understanding (*e.g.*, “*door*”).

## Task Setting and Benchmark

### Task Formulation

**OV-3D.** Let  $P = \{p_n\}_{n=1}^N \in \mathbb{R}^{N \times 3}$  represent 3D scenes with  $N$  points,  $I = \{i_x\}_{x=1}^X \in \mathbb{R}^{H \times W \times 3}$  denote  $X$  RGB image frames, and  $V = \{c_t\}_{t=1}^T$  is a vocabulary set of  $T$  text sentences, each describing the object class  $c_t$  that we aim to detect. An OV-3D model,  $\mathbb{M}$ , generates predictions with high confidence scores,  $Q = \mathbb{M}(P, I, V)$ . Predictions  $Q$  are then compared with the GT label  $G$  for evaluation.

**GOV-3D.** The existing 3D scene understanding benchmark, denoted as  $\mathcal{D} = \{(o_k, c_k)\}_{k=1}^K$ , comprises a collection of  $K$  object-label pairs. Each pair consists of an object  $o_k$  represented as a 3D mask and its corresponding class la-

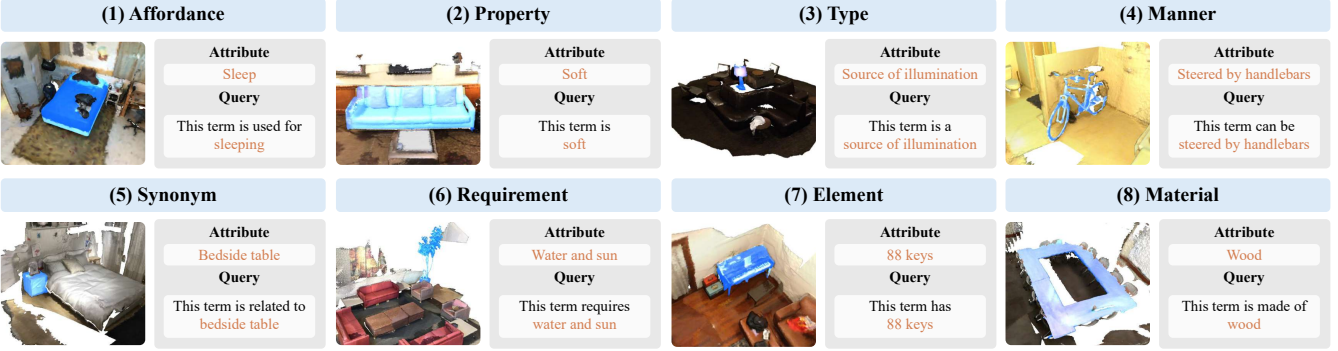


Figure 2: OpenScan benchmark samples. The target objects are highlighted in blue.

bel  $c_k$ . The benchmark is composed of multiple 3D scenes  $P = \{p_n\}_{n=1}^N \in \mathbb{R}^{N \times 3}$  with  $N$  points, and  $X$  RGB image frames  $I = \{i_x\}_{x=1}^X \in \mathbb{R}^{H \times W \times 3}$ . Building upon this, GOV-3D extends the class label  $c_k$  to object attribute  $a_k$ . Accordingly, the attribute set for 3D scenes  $P$  is defined as  $A = \{a_k\}_{k=1}^H$ , composed of  $H$  text sentences, each describing a specific attribute  $a_k$  that we aim to detect. A GOV-3D model,  $\mathbb{N}$ , produces predictions with high confidence scores,  $Q = \mathbb{N}(P, I, A)$ . The evaluation of the GOV-3D task involves comparing the predictions  $Q$  with the GT label  $G$ .

## Benchmark Description

The OpenScan benchmark is constructed based on the ScanNet200 (Rozenberszki et al. 2022) benchmark, which consists of 200 object classes with more than 1,500 3D scans. Since the ScanNet200 benchmark contains only an object-level class annotation for each object, it is not suitable for our GOV-3D task. To perform the GOV-3D task, we construct the OpenScan benchmark by leveraging the object annotations of the ScanNet benchmark. Our OpenScan provides attribute annotations for each object, expanding the single category of object classes in ScanNet200 into eight linguistic aspects of object-related attributes, including *affordance*, *property*, *type*, *manner*, *synonym*, *requirement*, *element*, and *material*. Figure 2 shows an example from our OpenScan benchmark. The target objects in our OpenScan are annotated with eight linguistic aspects of object attributes. The explanations of these eight object attributes are as follows:

- **Affordance:** is the object function or usage (e.g., “sit” for a chair).
- **Property:** indicates the object characteristic (e.g., “soft” for a pillow).
- **Type:** indicates the object category or group (e.g., “a communication device” for a telephone).
- **Manner:** indicates the object behavior (e.g., “worn on a head” for a hat).
- **Synonym:** is a term with a similar meaning (e.g., “image” for a picture).
- **Requirement:** indicates an essential condition that an object should possess to fulfill a specific need (e.g., “balance to ride” for a bicycle).
- **Element:** indicates an individual component or part that constitutes the object (e.g., “two wheels” for a bicycle).

- **Material:** indicates the type of material of the object (e.g., “plastic” for a bottle).

## Benchmark Annotation

Figure 3 illustrates the annotation process of our OpenScan benchmark. We first leverage the knowledge graph to establish the association between objects and various attributes. We also conduct manual annotations to label the visual attributes of each object. Finally, we classify and verify these attributes to ensure semantic consistency.

**Object-Attribute Association with Knowledge Graph.** We associate each object with various attributes using knowledge graphs, as illustrated in Figure 3. Let  $\mathcal{D} = \{(p_k, c_k)\}_{k=1}^K$  denotes the existing 3D scene understanding benchmark, e.g., ScanNet200 (Rozenberszki et al. 2022) in our implementation, where  $p_k$  is a target object,  $c_k$  is the corresponding class label, and  $K$  denotes the number of target object and label pairs. The benchmark is composed of multiple 3D scenes  $P \in \mathbb{R}^{N \times 3}$  with  $N$  points. Let  $\mathcal{G} = (\mathcal{V}, \mathcal{E})$  denotes the knowledge graph, where  $\mathcal{V}$  is the node set and  $\mathcal{E}$  is the edge set. The nodes  $v \in \mathcal{V}$  are natural language words and phrases, and the edges  $e \in \mathcal{E}$  are relation knowledge connecting them. Each edge  $e$  is directional, and can be represented as a tuple  $(v_m, r, w, v_n)$ , where  $v_m, v_n \in \mathcal{V}$  are the names of the head node and the tail node,  $r$  is the relation, and  $w$  is the importance weight of this relation. We extract the relation knowledge from the popular and high-quality NLP knowledge base ConceptNet (Speer, Chin, and Havasi 2017). An example of relation knowledge from it is:

$$e = (“bed”, “is used for”, 2.0, “sleep”). \quad (1)$$

We query a set of relation knowledge  $\{e\}_i$  linked to object class  $c_i$  from the knowledge graph  $\mathcal{G}$ . Formally, for each edge within it, the head node name is the same as the input object class, i.e.,  $v_m = c_i$ . The query process is defined as:

$$\{e\}_i = \{(v_m, r, w, v_n) \in \mathcal{E} | v_m = c_i\}. \quad (2)$$

**Attribute Selection.** In the set of relation knowledge  $\mathcal{E}$ , we keep the attribute with the highest weight  $w$  in the same relation  $r$ . Given a relation knowledge  $e_i \in \{e\}$ , we have:

$$\{e\}'_i = \{e_i | r_j = r_i \wedge \forall e_j \in \{e\} : w_j \leq w_i\}. \quad (3)$$

These object-attribute pairs form the basic annotations of OpenScan, which is useful in the GOV-3D task. Finally, each

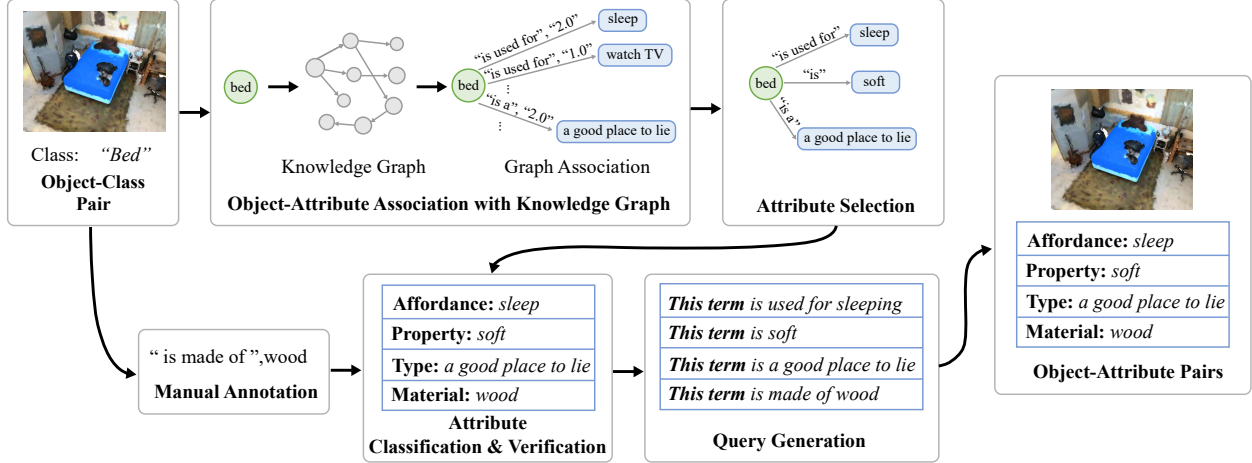


Figure 3: Illustration of the data generation process for our OpenScan benchmark.

3D object  $p_i$  is assigned a relation knowledge  $e_i$  through  $I$  annotations, serving as commonsense knowledge  $\mathcal{Y}_c$  as:

$$\mathcal{Y}_c = \{(p_i, e_i), e_i \in \{e\}' | v_m = c_i\}_i^I. \quad (4)$$

**Manual Annotation.** For the visual attribute that cannot be inferred without human perception, we manually annotate each 3D object following a rigorous protocol. We create a web interface for annotators to select each object’s visual attribute. Specifically, for each scene, annotators view the 3D point cloud and the target’s corresponding 2D image. Taking the *material* attribute as an example, annotators are tasked with identifying the primary material composition of the target object. Any 3D object with an ambiguous appearance is carefully identified through different camera views of the scene and the corresponding image frames around the object. Finally, each 3D object  $p_j$  is assigned with a relation  $r_j = \text{“is made of”}$  and a visual attribute like *material*  $v_n$  through  $J$  annotations, serving as visual appearance  $\mathcal{Y}_m$  in:

$$\mathcal{Y}_m = \{(p_j, (r_j, v_n))\}_j^J. \quad (5)$$

After obtaining the attribute annotations based on commonsense knowledge  $\mathcal{Y}_c$  and visual appearance  $\mathcal{Y}_m$  of the 3D objects, we use the combination of these two categories of attributes as the whole annotations  $\mathcal{Y}$  for our OpenScan.

**Attribute Classification.** To better organize our benchmark, we manually group each attribute into eight linguistic aspects based on relation  $r$  and attribute  $v_n$ . This process involves considering the nature of the relation  $r$  and attribute  $v_n$ , and how they align with each linguistic aspect. Subsequently, each attribute  $v_n$  is assigned to a linguistic aspect.

**Attribute Verification.** After the initial attribute classification, we manually verify each 3D object  $p_k$  with its corresponding attribute  $v_n$  and linguistic aspect. If a 3D object  $p_k$  contains multiple attributes  $v_n$  within a single linguistic aspect, we manually assign the most representative attribute to ensure evaluation consistency. This attribute is uniquely tied to the object class of  $p_k$  to eliminate cross-class ambiguity. We also filter out similar attributes  $v_n$  (e.g., “store things” and “store somethings”), preserving only one attribute to ensure consistency. During the verification process, the attributes across eight linguistic aspects are reduced from 528 to 341.

**Query Generation.** A practical GOV-3D query should incorporate attribute names but exclude object names, requiring a query strategy that focuses on attributes rather than exposing object identities (i.e., object classes). To achieve this, we perform query generation by hiding the object class  $v_m$  of the object  $p_k$ . We first replace the object classes  $v_m$  with a substitution term  $t = \text{“this term”}$ . The substitution term  $t$ , the relation  $r$ , and the corresponding attribute  $v_n$  are then concatenated to form the text query  $q$  as:

$$q = \text{Concat}(t, r, v_n). \quad (6)$$

In this way, we generate text queries  $q$  that correspond to object-attribute annotations  $\mathcal{Y}$ . We then perform manual verification again on text queries. With text queries as input, we can conduct evaluations on existing OV-3D models.

## Benchmark Statistics

Table 1 shows the statistics of our OpenScan benchmark. We have collected eight linguistic aspects of attributes, providing a total of 153,644 attribute annotations across 341 attributes for 1,513 scenes in ScanNet200 (Rozenberszki et al. 2022). In these aspects, the visual aspect of *material* is annotated manually, while other attributes are automatically generated via knowledge graph. There are 101.55 attribute annotations per scene in 1,513 3D indoor scenes. Besides, each object is annotated with an average of 3.15 attributes, indicating that most objects in ScanNet200 receive multiple attribute labels and are comprehensively represented. While certain linguistic aspects such as *manner* and *synonym* encompass a limited number of attributes, others like *affordance* and *type* consist of a wide range of attributes. We follow the training and validation split settings of ScanNet200.

## Evaluation Metrics

We employ commonly used OV-3D metrics to evaluate our GOV-3D task. For semantic segmentation, we follow (Peng et al. 2023; Ding et al. 2023; Yang et al. 2024) to apply mean IoU (mIoU) and mean accuracy (mAcc). For instance segmentation, we follow (Takmaz et al. 2023; Yin et al. 2024; Yan et al. 2024; Nguyen et al. 2024) to apply average precision (AP) at IoU scores of 25% (AP<sub>25</sub>), 50% (AP<sub>50</sub>), and the

Statistics	Affordance	Property	Type	Manner	Synonym	Requirement	Element	Material	All
Attributes	104	19	96	21	16	28	47	10	341
Attribute Annotations	37,362	8,591	28,293	4,925	2,937	9,695	13,505	48,336	153,644
Attribute Annotations per Object	0.77	0.18	0.58	0.10	0.06	0.20	0.28	0.99	3.15
Attribute Annotations per Scene	24.69	5.68	18.70	3.26	1.94	6.41	8.93	31.95	101.55

Table 1: OpenScan benchmark statistics of object-related attributes for the eight linguistic aspects.

Model	Training	Pre-Trained 3D Proposal	Pre-Trained 2D Proposal
OpenMask3D	-	Mask3D	SAM
SAI3D	-	-	Semantic-SAM
MaskClustering	-	-	CropFormer
Open3DIS	-	ISBNet	Grounded-SAM
OpenScene	-	-	-
PLA	ScanNet	-	-
RegionPLC	ScanNet	-	-

Table 2: The detailed information of the OV-3D models.

mean of AP from 50% to 95% at 5% steps. We compute the mean score (Mean) across all attributes to obtain the overall performance.

## Experiments

We conduct our experiments on the validation set of our OpenScan across eight linguistic aspects using the publicly available OV-3D models. All OV-3D models are evaluated in a zero-shot setting without training on the OpenScan benchmark. For 3D instance segmentation, we evaluate OpenMask3D (Takmaz et al. 2023), SAI3D (Yin et al. 2024), MaskClustering (Yan et al. 2024), and Open3DIS (Nguyen et al. 2024). For 3D semantic segmentation, we evaluate OpenScene (Peng et al. 2023), PLA (Ding et al. 2023), and RegionPLC (Yang et al. 2024). Table 2 summarizes the information of these models: the training set, pre-trained 3D proposal, and pre-trained 2D proposal. All experiments are conducted on one NVIDIA RTX 4090 GPU.

## Main Results

**3D Instance Segmentation.** We evaluate OpenMask3D (Takmaz et al. 2023), SAI3D (Yin et al. 2024), MaskClustering (Yan et al. 2024), and Open3DIS (Nguyen et al. 2024) across 341 attributes from our OpenScan and 198 object classes from ScanNet200 (Rozenberszki et al. 2022). Table 3 show that the performance of these OV-3D models on our GOV-3D benchmark, OpenScan, are significantly lower than those on the classic OV-3D dataset, ScanNet200. This gap underscores that our proposed GOV-3D task is a more challenging extension of the traditional OV-3D task.

When comparing the results of each OV-3D model across different linguistic aspects, we observe higher performances in the *synonym* and *material* aspects but struggle in the *affordance* and *property* aspects. The high performance in the *synonym* aspect can be attributed to the close similarity between attributes in this aspect and object classes, making recognition easier compared to the more abstract *affordance* and *property* aspects. An example of these closely related terms is shown in Figure 2, where the corresponding *synonym* aspect of the object class “nightstand” is “bedside table”. The high performance in the *material* aspect highlights the ability

of these OV-3D models to recognize visual patterns. By utilizing CLIP (Radford et al. 2021) for 3D scene understanding, these models benefit from its visual patterns, including material and color from image-text pretraining, enhancing their comprehension of visual attributes beyond other attributes.

When comparing the results of each linguistic aspect in our OpenScan to those of the object class in ScanNet200, we notice that certain aspects like *synonym* and *material* perform even better than the object class. This can be attributed to the smaller number of attributes in these two aspects when compared to the broader and more diverse set of object classes. A smaller set of classes can increase the model’s confidence in its predictions, facilitating more accurate predictions without the complexity of distinguishing among a large number of categories. Notably, Open3DIS shows impressive results in various linguistic aspects compared to other OV-3D models, aligning with its strong performances in the classic OV-3D task (*i.e.*, evaluating only on object classes).

**3D Semantic Segmentation.** We evaluate OpenScene (Peng et al. 2023), PLA (Ding et al. 2023), and RegionPLC (Yang et al. 2024), reporting the average score of all attributes in our OpenScan and that of all object classes in ScanNet (Dai et al. 2017). Table 4 shows that although these OV-3D models perform well in recognizing object classes, they exhibit poor performances on linguistic aspects with low mIoU and mAcc metrics. The methods for semantic segmentation suffer from a more significant performance drop on OpenScan when compared with those for instance segmentation. This drop can be caused by several factors. First, there is a significant discrepancy in the vocabulary size between ScanNet and our OpenScan. A larger vocabulary size implies a more diverse set of semantic concepts that the model needs to comprehend, making our OpenScan more challenging and practical in real-world scenarios. In addition, the arbitrary nature of object attributes in contrast to object classes adds complexity to the GOV-3D task. Besides, the lack of both robust 3D proposals (*e.g.*, Mask3D (Schult et al. 2023)) and 2D proposals (*e.g.*, SAM (Kirillov et al. 2023)) for class-agnostic masks can also be attributed to the drop. Conversely, instance segmentation models like OpenMask3D (Takmaz et al. 2023) leverage strong instance-level knowledge, *e.g.*, proposals extracted from Mask3D and SAM, to effectively segment novel 3D objects, leading to higher performances on the GOV-3D task.

## The Impact of the Pre-trained Vocabulary Size

To study the impact of the pre-trained vocabulary size (*i.e.*, the number of pre-trained object classes) on the GOV-3D task, we conduct experiments based on RegionPLC (Yang et al. 2024) for 3D semantic segmentation. Figure 4 reports the mIoU and mAcc scores under different pre-training vocabulary sizes  $S \in \{10, 12, 15, 150, 170\}$ , on the ScanNet (Dai et al. 2017) and ScanNet200 (Rozenberszki et al. 2022)

Method	OpenScan									ScanNet200
	Affordance	Property	Type	Manner	Synonym	Requirement	Element	Material	Mean	Object Class
AP										
OpenMask3D (Takmaz et al. 2023)	7.2	7.5	8.5	12.8	16.9	13.0	12.2	18.8	9.9	15.4
SAI3D (Yin et al. 2024)	5.3	5.8	7.8	11.3	10.0	10.0	8.7	11.3	7.7	12.7
MaskClustering (Yan et al. 2024)	6.2	7.0	7.1	11.1	16.2	11.3	7.4	12.1	8.1	12.0
Open3DIS (Nguyen et al. 2024)	<b>11.9</b>	<b>12.8</b>	<b>14.2</b>	<b>19.2</b>	<b>26.7</b>	<b>19.2</b>	<b>18.7</b>	<b>28.3</b>	<b>15.8</b>	<b>23.7</b>
AP <sub>50</sub>										
OpenMask3D (Takmaz et al. 2023)	9.1	10.0	11.2	15.4	19.7	16.0	15.4	22.1	12.5	19.9
SAI3D (Yin et al. 2024)	8.4	8.3	11.4	15.7	16.7	15.3	13.6	17.1	11.6	18.8
MaskClustering (Yan et al. 2024)	10.7	12.3	13.3	18.4	30.3	21.8	13.5	20.6	14.6	23.3
Open3DIS (Nguyen et al. 2024)	<b>14.8</b>	<b>16.0</b>	<b>17.9</b>	<b>22.3</b>	<b>30.6</b>	<b>24.1</b>	<b>21.9</b>	<b>33.6</b>	<b>19.3</b>	<b>29.4</b>
AP <sub>25</sub>										
OpenMask3D (Takmaz et al. 2023)	10.4	11.6	13.0	17.4	20.6	18.9	17.1	25.0	14.2	23.1
SAI3D (Yin et al. 2024)	10.5	10.7	13.4	18.2	20.0	18.7	16.0	22.9	14.1	24.1
MaskClustering (Yan et al. 2024)	13.7	15.8	17.7	23.1	<b>36.6</b>	<b>28.2</b>	17.2	25.6	18.7	30.1
Open3DIS (Nguyen et al. 2024)	<b>16.7</b>	<b>16.8</b>	<b>20.2</b>	<b>24.2</b>	33.1	25.5	<b>24.7</b>	<b>36.7</b>	<b>21.4</b>	<b>32.8</b>

Table 3: 3D instance segmentation results on our OpenScan benchmark.

Method	OpenScan		ScanNet	
	mIoU	mAcc	mIoU	mAcc
OpenScene (Peng et al. 2023)	<b>0.45</b>	1.87	47.5	70.7
PLA (Ding et al. 2023)	0.01	<b>2.37</b>	66.6	77.5
RegionPLC (Yang et al. 2024)	0.07	2.36	<b>68.7</b>	<b>78.7</b>

Table 4: 3D semantic segmentation results on OpenScan.

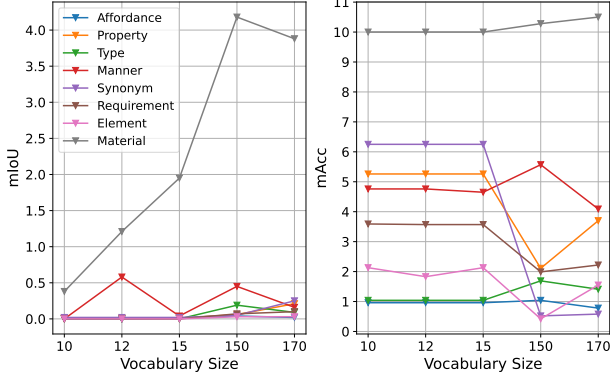


Figure 4: Impact of different pre-training vocabulary size.

datasets. Results show that the majority of the linguistic aspects of object attributes do not exhibit a notable enhancement as  $S$  increases, reflected by both mIoU and mAcc scores, aligning with our expectations. Some linguistic aspects of object attributes show relatively low performances and exhibit random jitters. Among the eight linguistic aspects, the aspect *material* illustrates an enhancement in mIoU and a marginal improvement in mAcc as  $S$  increases. This improvement can be attributed to the framework adopted by RegionPLC, which associates 3D objects with language through explicit visual image captioning models, providing detailed descriptions of visual attributes like material and color for each 3D object. Therefore, as the vocabulary size  $S$  increases, more objects are processed by the image captioning model to produce visual descriptions that ultimately improve the semantic segmentation results for the aspect *material*.

Method	Template	AP	AP <sub>50</sub>	AP <sub>25</sub>
OpenMask3D (Takmaz et al. 2023)	-	9.7	12.2	14.1
	✓	<b>9.9</b>	<b>12.5</b>	<b>14.2</b>
SAI3D (Yin et al. 2024)	-	6.7	10.1	12.8
	✓	<b>7.7</b>	<b>11.6</b>	<b>14.1</b>
MaskClustering (Yan et al. 2024)	-	6.8	12.0	14.6
	✓	<b>8.1</b>	<b>14.6</b>	<b>18.7</b>
Open3DIS (Nguyen et al. 2024)	-	15.6	19.2	21.3
	✓	<b>15.8</b>	<b>19.3</b>	<b>21.4</b>

Table 5: Effects of query form on our OpenScan benchmark.

This observation suggests that simply increasing the size of the object vocabulary during training may not effectively enhance the generalization capability of OV-3D models. This limitation can be attributed to existing OV-3D benchmarks, like ScanNet (Dai et al. 2017), ScanNet200 (Rozenberszki et al. 2022), and ScanNet++ (Yeshwanth et al. 2023), which primarily focus on object classes and lack object-related attributes. While increasing the size of the object vocabulary during training can improve the OV-3D performance, as demonstrated by the results from PLA (Ding et al. 2023) and RegionPLC (Yang et al. 2024), this approach is not suitable for the more challenging GOV-3D task. The significant performance gap between the two tasks cannot be resolved simply by transferring the OV-3D technique into GOV-3D.

## The Impact of the Query Form

In benchmark annotation, we generate queries linking attributes to object classes. An ideal query should contain an attribute name and the relation between the attribute and the corresponding object class. Table 5 shows the effect of using a query template (*e.g.*, “*this term is made of wood*”) versus a plain term (*e.g.*, “*wood*”) in GOV-3D. We evaluate the 3D instance segmentation of OpenMask3D (Takmaz et al. 2023), SAI3D (Yin et al. 2024), MaskClustering (Yan et al. 2024), and Open3DIS (Nguyen et al. 2024), reporting the mean score of all attributes in OpenScan. Note that, as expected, using the query template improves model performance, as shown

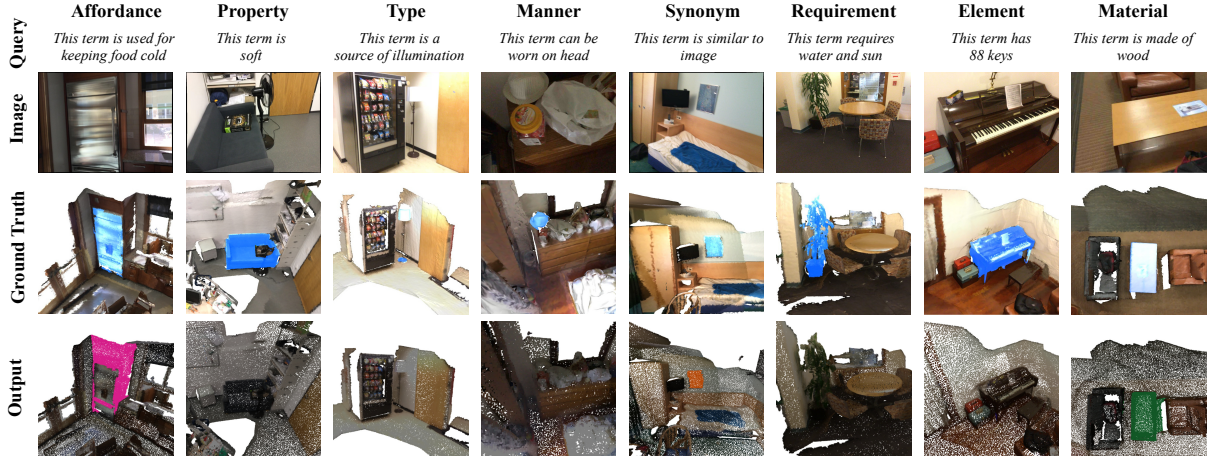


Figure 5: Qualitative results of Open3DIS on our OpenScan benchmark. The GT objects and outputs are highlighted in color.

by higher AP, AP<sub>50</sub>, and AP<sub>25</sub>. SAI3D and MaskClustering are more sensitive to query templates, while OpenMask3D and Open3DIS show greater robustness.

These results stem from the fact that VLMs, like CLIP (Radford et al. 2021), struggle with attribute classification in GOV-3D when minor commonsense knowledge is required, as stated in (Ye et al. 2023). Since most OV-3D models rely on VLMs like CLIP (Radford et al. 2021) for open-vocabulary comprehension, they inherit VLMs’ commonsense limitations. Thus, incorporating query templates that link attributes to object classes as commonsense knowledge improves OV-3D models’ performances in GOV-3D.

## Qualitative Results

We present qualitative results from Open3DIS (Nguyen et al. 2024) on our OpenScan benchmark. We evaluate Open3DIS across eight linguistic aspects, as shown in Figure 5. It demonstrates that Open3DIS can comprehend specific linguistic aspects such as *synonym* and *material*. When exploring the *affordance* aspect by querying “*keep food cold*” for the target object, Open3DIS can successfully identify the “*refrigerator*” as the target object but struggles to generate a correct 3D mask. Additionally, Open3DIS fails to generate predictions for other linguistic aspects. These observations align with the quantitative results in Table 3.

## Failure Cases Analysis

Figure 6 shows a failure case of Open3DIS (Nguyen et al. 2024) when applied to GOV-3D, despite its strong performance on OV-3D. While Open3DIS correctly identifies the object class (e.g., “*piano*”), it fails to recognize the associated object attribute (e.g., “*this term has 88 keys*”). To investigate this discrepancy, we analyze the CLIP (Radford et al. 2021) image-text similarity scores in Open3DIS, given that most OV-3D models rely on VLMs like CLIP (Radford et al. 2021) for 3D predictions. Our analysis reveals that CLIP assigns lower image-text similarity scores to the object attribute compared to the object class, suggesting that its intrinsic attribute knowledge is limited. This observation demonstrates that GOV-3D presents greater challenges compared to OV-3D. A promising direction for GOV-3D involves integrating at-

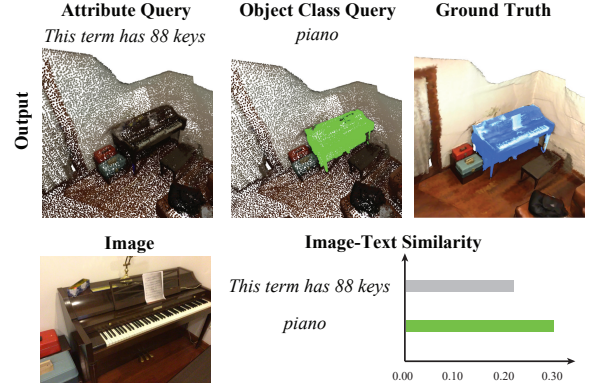


Figure 6: Visualization of the Open3DIS failure case with the corresponding CLIP image-text similarity scores.

tribute knowledge into VLMs like CLIP, which may improve image-text alignment and enable more reliable predictions.

## Conclusion

In this paper, we address the constraints of the classic Open-Vocabulary 3D Scene Understanding (OV-3D) task, which is limited in handling object attributes beyond object classes. We introduce a more challenging task, called Generalized Open-Vocabulary 3D Scene Understanding (GOV-3D), to comprehensively evaluate the generalization capability of OV-3D models. To facilitate research on the GOV-3D task, we construct a large-scale benchmark named OpenScan, which consists of 341 attributes across 8 linguistic aspects. We systematically evaluate the OV-3D models on the OpenScan benchmark, revealing their challenges in understanding attributes beyond object classes. We also conduct experiments to investigate the impact of the pre-trained vocabulary size and query form, demonstrating that the generalization ability can be enhanced by utilizing query templates rather than scaling up the vocabulary size during training. We further explore a promising direction for the GOV-3D task by integrating attribute knowledge into VLMs of the OV-3D models. We believe our OpenScan benchmark can facilitate future research on improving the generalization capability of OV-3D models.

## References

Armeni, I.; Sener, O.; Zamir, A. R.; Jiang, H.; Brilakis, I.; Fischer, M.; and Savarese, S. 2016. 3d semantic parsing of large-scale indoor spaces. In *Proceedings of the IEEE/CVF Conference on Computer Vision and Pattern Recognition*, 1534–1543.

Baruch, G.; Chen, Z.; Dehghan, A.; Dimry, T.; Feigin, Y.; Fu, P.; Gebauer, T.; Joffe, B.; Kurz, D.; Schwartz, A.; and Shulman, E. 2021. ARKitScenes - A Diverse Real-World Dataset for 3D Indoor Scene Understanding Using Mobile RGB-D Data. In *Thirty-fifth Conference on Neural Information Processing Systems Datasets and Benchmarks Track (Round 1)*.

Bianchi, L.; Carrara, F.; Messina, N.; Gennaro, C.; and Falchi, F. 2024. The devil is in the fine-grained details: Evaluating open-vocabulary object detectors for fine-grained understanding. In *Proceedings of the IEEE/CVF Conference on Computer Vision and Pattern Recognition*, 22520–22529.

Bojarski, M.; Del Testa, D.; Dworakowski, D.; Firner, B.; Flepp, B.; Goyal, P.; Jackel, L. D.; Monfort, M.; Muller, U.; Zhang, J.; et al. 2016. End to end learning for self-driving cars. *arXiv:1604.07316*.

Chang, A.; Dai, A.; Funkhouser, T.; Halber, M.; Niessner, M.; Savva, M.; Song, S.; Zeng, A.; and Zhang, Y. 2017. Matterport3D: Learning from RGB-D Data in Indoor Environments. *International Conference on 3D Vision*.

Chen, D. Z.; Chang, A. X.; and Nießner, M. 2020. Scanrefer: 3d object localization in rgb-d scans using natural language. In *European Conference on Computer Vision*, 202–221. Springer.

Chiang, W.-L.; Li, Z.; Lin, Z.; Sheng, Y.; Wu, Z.; Zhang, H.; Zheng, L.; Zhuang, S.; Zhuang, Y.; Gonzalez, J. E.; Stoica, I.; and Xing, E. P. 2023. Vicuna: An Open-Source Chatbot Impressing GPT-4 with 90%\* ChatGPT Quality.

Choy, C.; Gwak, J.; and Savarese, S. 2019. 4d spatio-temporal convnets: Minkowski convolutional neural networks. In *Proceedings of the IEEE/CVF Conference on Computer Vision and Pattern Recognition*, 3075–3084.

Cordts, M.; Omran, M.; Ramos, S.; Rehfeld, T.; Enzweiler, M.; Benenson, R.; Franke, U.; Roth, S.; and Schiele, B. 2016. The cityscapes dataset for semantic urban scene understanding. In *Proceedings of the IEEE Conference on Computer Vision and Pattern Recognition*, 3213–3223.

Dai, A.; Chang, A. X.; Savva, M.; Halber, M.; Funkhouser, T.; and Nießner, M. 2017. Scannet: Richly-annotated 3d reconstructions of indoor scenes. In *Proceedings of the IEEE Conference on Computer Vision and Pattern Recognition*, 5828–5839.

Delitzas, A.; Takmaz, A.; Tombari, F.; Sumner, R.; Pollefeys, M.; and Engelmann, F. 2024. Scenefun3d: Fine-grained functionality and affordance understanding in 3d scenes. In *Proceedings of the IEEE/CVF Conference on Computer Vision and Pattern Recognition*, 14531–14542.

Ding, R.; Yang, J.; Xue, C.; Zhang, W.; Bai, S.; and Qi, X. 2023. PLA: Language-Driven Open-Vocabulary 3D Scene Understanding. In *Proceedings of the IEEE/CVF Conference on Computer Vision and Pattern Recognition*, 7010–7019.

Ester, M.; Kriegel, H.-P.; Sander, J.; and Xu, X. 1996. A density-based algorithm for discovering clusters in large spatial databases with noise. In *Proceedings of the Second International Conference on Knowledge Discovery and Data Mining*, KDD'96, 226–231. AAAI Press.

Everingham, M.; Eslami, S. A.; Van Gool, L.; Williams, C. K.; Winn, J.; and Zisserman, A. 2015. The pascal visual object classes challenge: A retrospective. *International Journal of Computer Vision*, 111: 98–136.

Ghiasi, G.; Gu, X.; Cui, Y.; and Lin, T.-Y. 2022. Scaling open-vocabulary image segmentation with image-level labels. In *European Conference on Computer Vision*, 540–557. Springer.

Graham, B.; Engelcke, M.; and Van Der Maaten, L. 2018. 3d semantic segmentation with submanifold sparse convolutional networks. In *Proceedings of the IEEE/CVF Conference on Computer Vision and Pattern Recognition*, 9224–9232.

Gu, X.; Lin, T.-Y.; Kuo, W.; and Cui, Y. 2022. Open-vocabulary Object Detection via Vision and Language Knowledge Distillation. In *International Conference on Learning Representations*.

Gupta, A.; Dollar, P.; and Girshick, R. 2019. LvIs: A dataset for large vocabulary instance segmentation. In *Proceedings of the IEEE/CVF Conference on Computer Vision and Pattern Recognition*, 5356–5364.

Huang, K.-C.; Li, X.; Qi, L.; Yan, S.; and Yang, M.-H. 2025. Reason3d: Searching and reasoning 3d segmentation via large language model. In *International Conference on 3D Vision 2025*.

Huang, Z.; Wu, X.; Chen, X.; Zhao, H.; Zhu, L.; and Lasenby, J. 2024. Openins3d: Snap and lookup for 3d open-vocabulary instance segmentation. In *European Conference on Computer Vision*, 169–185. Springer.

Kirillov, A.; Mintun, E.; Ravi, N.; Mao, H.; Rolland, C.; Gustafson, L.; Xiao, T.; Whitehead, S.; Berg, A. C.; Lo, W.-Y.; Dollar, P.; and Girshick, R. 2023. Segment Anything. In *Proceedings of the IEEE/CVF International Conference on Computer Vision*, 4015–4026.

Li, F.; Zhang, H.; Sun, P.; Zou, X.; Liu, S.; Li, C.; Yang, J.; Zhang, L.; and Gao, J. 2024. Segment and recognize anything at any granularity. In *European Conference on Computer Vision*, 467–484. Springer.

Lin, T.-Y.; Maire, M.; Belongie, S.; Hays, J.; Perona, P.; Ramanan, D.; Dollár, P.; and Zitnick, C. L. 2014. Microsoft coco: Common objects in context. In *European Conference on Computer Vision*, 740–755. Springer.

Liu, S.; Zeng, Z.; Ren, T.; Li, F.; Zhang, H.; Yang, J.; Jiang, Q.; Li, C.; Yang, J.; Su, H.; et al. 2024. Grounding dino: Marrying dino with grounded pre-training for open-set object detection. In *European Conference on Computer Vision*, 38–55. Springer.

Lu, S.; Chang, H.; Jing, E. P.; Bouliarias, A.; and Bekris, K. 2023. Ovir-3d: Open-vocabulary 3d instance retrieval without training on 3d data. In *Conference on Robot Learning*, 1610–1620. PMLR.

Lyu, R.; Lin, J.; Wang, T.; Mao, X.; Chen, Y.; Xu, R.; Huang, H.; Zhu, C.; Lin, D.; and Pang, J. 2024. Mmscan: A multi-modal 3d scene dataset with hierarchical grounded language annotations. *Advances in Neural Information Processing Systems*, 37: 50898–50924.

Ngo, T. D.; Hua, B.-S.; and Nguyen, K. 2023. ISBNet: A 3D Point Cloud Instance Segmentation Network With Instance-Aware Sampling and Box-Aware Dynamic Convolution. In *Proceedings of the IEEE/CVF Conference on Computer Vision and Pattern Recognition*, 13550–13559.

Nguyen, P.; Ngo, T. D.; Kalogerakis, E.; Gan, C.; Tran, A.; Pham, C.; and Nguyen, K. 2024. Open3dis: Open-vocabulary 3d instance segmentation with 2d mask guidance. In *Proceedings of the IEEE/CVF Conference on Computer Vision and Pattern Recognition*, 4018–4028.

Peng, S.; Genova, K.; Jiang, C.; Tagliasacchi, A.; Pollefeys, M.; Funkhouser, T.; et al. 2023. Openscene: 3d scene understanding with open vocabularies. In *Proceedings of the IEEE/CVF Conference on Computer Vision and Pattern Recognition*, 815–824.

Qi, L.; Kuen, J.; Shen, T.; Gu, J.; Li, W.; Guo, W.; Jia, J.; Lin, Z.; and Yang, M.-H. 2023. High Quality Entity Segmentation. In *2023 IEEE/CVF International Conference on Computer Vision*, 4024–4033.

Radford, A.; Kim, J. W.; Hallacy, C.; Ramesh, A.; Goh, G.; Agarwal, S.; Sastry, G.; Askell, A.; Mishkin, P.; Clark, J.; et al. 2021. Learning transferable visual models from natural language supervision. In *International Conference on Machine Learning*, 8748–8763. PMLR.

Ramanathan, V.; Kalia, A.; Petrovic, V.; Wen, Y.; Zheng, B.; Guo, B.; Wang, R.; Marquez, A.; Kovvuri, R.; Kadian, A.; et al. 2023. Paco: Parts and attributes of common objects. In *Proceedings of the IEEE/CVF Conference on Computer Vision and Pattern Recognition*, 7141–7151.

Ren, T.; Liu, S.; Zeng, A.; Lin, J.; Li, K.; Cao, H.; Chen, J.; Huang, X.; Chen, Y.; Yan, F.; et al. 2024. Grounded sam: Assembling open-world models for diverse visual tasks. *arXiv:2401.14159*.

Rozenberszki, D.; Litany, O.; Dai, A.; and Dai, A. 2022. Language-Grounded Indoor 3D Semantic Segmentation in the Wild. In *Proceedings of the European Conference on Computer Vision*.

Schult, J.; Engelmann, F.; Hermans, A.; Litany, O.; Tang, S.; and Leibe, B. 2023. Mask3D: Mask Transformer for 3D Semantic Instance Segmentation. In *2023 IEEE International Conference on Robotics and Automation*, 8216–8223.

Speer, R.; Chin, J.; and Havasi, C. 2017. Conceptnet 5.5: An open multilingual graph of general knowledge. In *Proceedings of the AAAI Conference on Artificial Intelligence*, volume 31.

Straub, J.; Whelan, T.; Ma, L.; Chen, Y.; Wijmans, E.; Green, S.; Engel, J. J.; Mur-Artal, R.; Ren, C.; Verma, S.; et al. 2019. The Replica dataset: A digital replica of indoor spaces. *arXiv:1906.05797*.

Takmaz, A.; Fedele, E.; Sumner, R. W.; Pollefeys, M.; Tombari, F.; and Engelmann, F. 2023. OpenMask3D: Open-Vocabulary 3D Instance Segmentation. In *Advances in Neural Information Processing Systems*.

Xu, W.; Shi, C.; Tu, S.; Zhou, X.; Liang, D.; and Bai, X. 2024. A Unified Framework for 3D Scene Understanding. In *Advances in Neural Information Processing Systems*.

Yan, M.; Zhang, J.; Zhu, Y.; and Wang, H. 2024. Maskclustering: View consensus based mask graph clustering for open-vocabulary 3d instance segmentation. In *Proceedings of the IEEE/CVF Conference on Computer Vision and Pattern Recognition*, 28274–28284.

Yang, J.; Ding, R.; Deng, W.; Wang, Z.; and Qi, X. 2024. Regionplc: Regional point-language contrastive learning for open-world 3d scene understanding. In *Proceedings of the IEEE/CVF Conference on Computer Vision and Pattern Recognition*, 19823–19832.

Yao, Y.; Liu, P.; Zhao, T.; Zhang, Q.; Liao, J.; Fang, C.; Lee, K.; and Wang, Q. 2024. How to Evaluate the Generalization of Detection? A Benchmark for Comprehensive Open-Vocabulary Detection. In *Proceedings of the AAAI Conference on Artificial Intelligence*, volume 38, 6630–6638.

Ye, S.; Xie, Y.; Chen, D.; Xu, Y.; Yuan, L.; Zhu, C.; and Liao, J. 2023. Improving commonsense in vision-language models via knowledge graph riddles. In *Proceedings of the IEEE/CVF Conference on Computer Vision and Pattern Recognition*, 2634–2645.

Yeshwanth, C.; Liu, Y.-C.; Nießner, M.; and Dai, A. 2023. ScanNet++: A high-fidelity dataset of 3d indoor scenes. In *Proceedings of the IEEE/CVF International Conference on Computer Vision*, 12–22.

Yin, Y.; Liu, Y.; Xiao, Y.; Cohen-Or, D.; Huang, J.; and Chen, B. 2024. Sai3d: Segment any instance in 3d scenes. In *Proceedings of the IEEE/CVF Conference on Computer Vision and Pattern Recognition*, 3292–3302.

Zeng, A.; Song, S.; Welker, S.; Lee, J.; Rodriguez, A.; and Funkhouser, T. 2018. Learning synergies between pushing and grasping with self-supervised deep reinforcement learning. In *2018 IEEE/RSJ International Conference on Intelligent Robots and Systems*, 4238–4245. IEEE.

Zhao, Y.; Lin, J.; and Lau, R. W. 2025. Hierarchical Cross-Modal Alignment for Open-Vocabulary 3D Object Detection. In *Proceedings of the AAAI Conference on Artificial Intelligence*, volume 39, 10501–10509.

Zhong, Y.; Yang, J.; Zhang, P.; Li, C.; Codella, N.; Li, L. H.; Zhou, L.; Dai, X.; Yuan, L.; Li, Y.; et al. 2022. Regionclip: Region-based language-image pretraining. In *Proceedings of the IEEE/CVF Conference on Computer Vision and Pattern Recognition*, 16793–16803.

Zhou, B.; Zhao, H.; Puig, X.; Xiao, T.; Fidler, S.; Barriuso, A.; and Torralba, A. 2019. Semantic understanding of scenes through the ade20k dataset. *International Journal of Computer Vision*, 127: 302–321.

# Supplementary Material

In this supplementary material, we provide more experimental results and benchmark details:

- Sec. A: Web interface for manual annotation.
- Sec. B: Implementation details.
- Sec. C: Additional experimental results.
- Sec. D: Additional benchmark details.
- Sec. E: Additional related work.
- Sec. F: Limitations and future work.
- Sec. G: Broader impact.

## A Web Interface for Manual Annotation

We implement a web interface for manual annotation of the visual linguistic aspect (*e.g.*, *material*), as shown in Figure A. Annotators are shown an interactive 3D mesh of a scene, a list of target objects, and a list of attributes. Users can control the 3D mesh from different viewpoints interactively by rotating, zooming in, zooming out, and panning to observe the scene from various viewpoints. When users select a 3D mesh by clicking the mouse in the scene, the target object will be highlighted and the corresponding object ID and object class will be displayed. The annotation process requires annotators to first select a target object in the 3D mesh (*e.g.*, table of ID 2) and then select a primary attribute that belongs to the target object (*e.g.*, stone). Finally, annotators click the confirm button to submit and store the annotations. Once the selected objects are annotated and confirmed, the corresponding object in the object list will show a check mark symbol. Additionally, to address visual ambiguity issues in 3D object appearance, our annotation process allows users to review the scene’s video sequences, providing contextual visual cues to resolve uncertainties about target objects’ visual attributes during annotation.

## B Implementation Details

### B.1 Open-Vocabulary 3D Scene Understanding (OV-3D) Baselines

We report implementation details of the OV-3D models (Takmaz et al. 2023; Yin et al. 2024; Yan et al. 2024; Nguyen et al. 2024; Peng et al. 2023; Ding et al. 2023; Yang et al. 2024) as follows:

**OpenMask3D.** In the class-agnostic mask proposal module, we employ the Mask3D (Schult et al. 2023) architecture trained on the ScanNet200 (Rozenberszki et al. 2022) training set. For 2D mask proposals, we use SAM (Kirillov et al. 2023) with ViT-H as the backbone. We utilize the pre-trained CLIP (Radford et al. 2021) visual encoder of ViT-L/14 at a 336 pixel resolution to extract image features with 768 dimensions. We set the number of queries to 150, following the implementation of OpenMask3D (Takmaz et al. 2023) and Mask3D (Schult et al. 2023), to ensure a sufficient number of mask proposals for the GOV-3D task.

**SAI3D.** We employ Semantic-SAM (Li et al. 2024) with Swin-L as the backbone to generate 2D mask proposals. The number of queries is set to 150 to ensure sufficient mask proposals for the GOV-3D task.



Figure A: Web interface for manual annotation that allows users to view the 3D scene from multiple viewpoints and select the target object by clicking.

**MaskClustering.** We utilize CropFormer (Qi et al. 2023) as a 2D mask predictor. For 2D mask proposals, we use CLIP (Radford et al. 2021) visual encoder of ViT-H/14 to extract image features. We follow MaskClustering (Yan et al. 2024) to adopt the post-processing approach from OVR-3D (Lu et al. 2023) to refine the output 3D instances. Specifically, we employ the DBSCAN (Ester et al. 1996) algorithm to partition disconnected point clusters.

**Open3DIS.** We utilize the class-agnostic 3D proposal network ISBNet (Ngo, Hua, and Nguyen 2023) trained on the ScanNet200 (Rozenberszki et al. 2022) training set as 3D proposal. We employ the 2D-Guided-3D Instance Proposal Module in Open3DIS (Nguyen et al. 2024). For 2D mask proposals, we adopt Grounded-SAM (Ren et al. 2024) as 2D segmentor, which incorporates a Swin-T-based Grounding-DINO (Liu et al. 2024) decoder and SAM (Kirillov et al. 2023) with ViT-H as the backbone.

**OpenScene.** We employ OpenSeg (Ghiasi et al. 2022) for image feature extraction and a 2D-3D ensemble model in OpenScene (Peng et al. 2023). We utilize MinkowskiNet18A (Choy, Gwak, and Savarese 2019) as the 3D backbone during 3D distillation.

**PLA.** We utilize a model trained on the ScanNet (Dai et al. 2017) partition of B15/N4, where B15/N4 indicates 15 base and 4 novel categories. We adopt a SparseUNet16 architecture based on sparse convolutions UNet (Graham, Engelcke, and Van Der Maaten 2018) as our 3D encoder for semantic segmentation and integrate the CLIP (Radford et al. 2021) text encoder as the final classifier.

**RegionPLC.** We utilize a model trained on the ScanNet (Dai et al. 2017) partition of B15/N4, where B15/N4 represents 15 base and 4 novel categories. We employ a sparse-convolution-based UNet (Graham, Engelcke, and Van Der Maaten 2018) of SparseUNet16 as the 3D encoder for semantic segmentation, leveraging the CLIP (Radford et al. 2021) text encoder as the final classifier.

### B.2 Evaluation Protocol

We evaluate the OV-3D baselines on 312 scenes following the validation split of ScanNet200 (Rozenberszki et al. 2022)

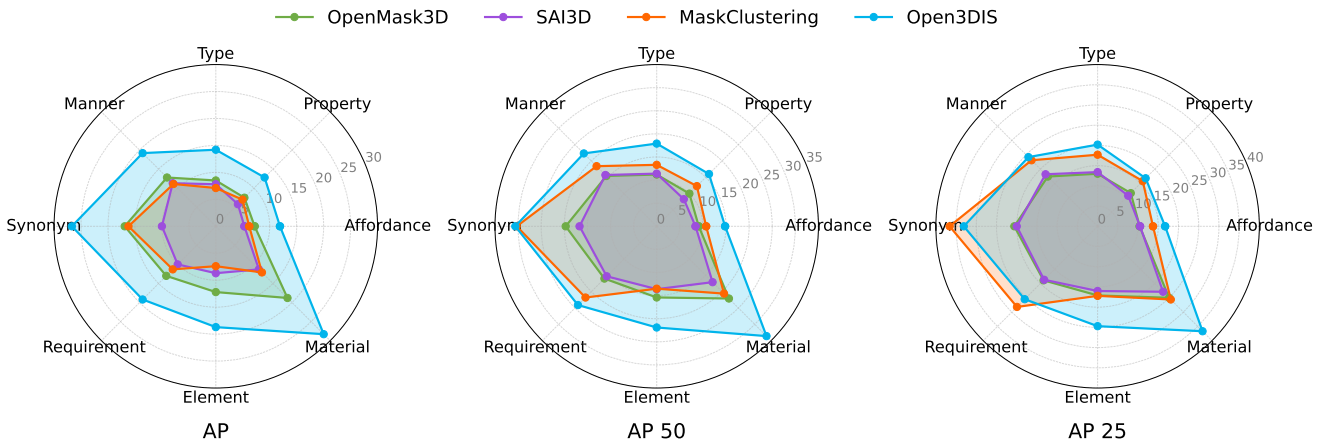


Figure B: Radar charts of AP, AP<sub>50</sub>, and AP<sub>25</sub> results for eight linguistic aspects on our OpenScan benchmark.

Method	Affordance	Property	Type	Manner	Synonym	Requirement	Element	Material	Mean
<b>AP</b>									
OpenMask3D (Takmaz et al. 2023)	7.7	8.2	8.7	14.2	16.3	12.0	10.0	14.7	9.7
SAI3D (Yin et al. 2024)	4.0	5.5	7.4	10.6	8.6	8.8	7.3	8.3	6.7
MaskClustering (Yan et al. 2024)	6.0	6.2	4.1	8.0	11.7	10.3	9.3	8.1	6.8
Open3DIS (Nguyen et al. 2024)	<b>11.5</b>	<b>17.6</b>	<b>14.5</b>	<b>18.5</b>	<b>27.7</b>	<b>18.6</b>	<b>16.6</b>	<b>23.4</b>	<b>15.6</b>
<b>AP<sub>50</sub></b>									
OpenMask3D (Takmaz et al. 2023)	9.6	10.7	11.2	18.1	18.4	15.2	12.8	17.8	12.2
SAI3D (Yin et al. 2024)	6.4	8.2	10.6	14.9	13.0	13.8	11.5	13.3	10.1
MaskClustering (Yan et al. 2024)	10.3	11.5	7.2	13.5	23.1	18.7	16.1	14.0	12.0
Open3DIS (Nguyen et al. 2024)	<b>14.3</b>	<b>22.2</b>	<b>18.3</b>	<b>22.6</b>	<b>32.9</b>	<b>23.1</b>	<b>19.7</b>	<b>28.5</b>	<b>19.2</b>
<b>AP<sub>25</sub></b>									
OpenMask3D (Takmaz et al. 2023)	10.8	12.4	13.9	20.4	18.9	18.0	14.4	20.5	14.1
SAI3D (Yin et al. 2024)	8.5	11.1	13.1	18.6	15.9	17.5	14.7	18.6	12.8
MaskClustering (Yan et al. 2024)	12.3	13.5	9.4	16.9	25.1	24.1	19.0	18.1	14.6
Open3DIS (Nguyen et al. 2024)	<b>16.2</b>	<b>24.0</b>	<b>20.2</b>	<b>24.8</b>	<b>35.9</b>	<b>24.9</b>	<b>22.7</b>	<b>31.9</b>	<b>21.3</b>

Table A: 3D instance segmentation results without query template on our OpenScan benchmark.

dataset. Our evaluation includes all 341 attributes across 8 linguistic aspects.

## C Additional Experimental Results

### C.1 Results of Radar Charts.

Figure B presents radar charts of the main results on our OpenScan benchmark. The charts compare performance across AP, AP<sub>50</sub>, and AP<sub>25</sub> for OpenMask3D (Takmaz et al. 2023), SAI3D (Yin et al. 2024), MaskClustering (Yan et al. 2024), and Open3DIS (Nguyen et al. 2024). Our results demonstrate that Open3DIS achieves the strongest performance across eight linguistic aspects, particularly in terms of AP and AP<sub>50</sub>. Meanwhile, MaskClustering exhibits competitive performance in AP<sub>50</sub> and AP<sub>25</sub>, with notable strengths in the *synonym* and *requirement* aspects.

### C.2 Results Without Query Templates.

In this paper, we adopt query templates (e.g., “*this term is made of wood*”) as the default experimental configuration. For template-free evaluation on the GOV-3D benchmark (e.g., “*wood*”), detailed results are provided in Table A. We evaluate OpenMask3D (Takmaz et al. 2023), SAI3D (Yin et al. 2024), MaskClustering (Yan et al. 2024), and Open3DIS (Nguyen et al. 2024) for 3D instance segmentation. Our experiments show that Open3DIS achieves the highest AP, AP<sub>50</sub>, and AP<sub>25</sub> scores across every linguistic aspect. This performance aligns with its strong performance in the GOV-3D task with query templates.

### C.3 Results of Visual Attributes

We present comparative visual attribute results for the *material* aspect on our OpenScan benchmark in Table B. Our evaluation involves OpenMask3D (Takmaz et al. 2023), SAI3D (Yin et al. 2024), MaskClustering (Yan et al. 2024),

Method	Wood	Fabric	Leather	Cotton	Metal	Stone	Porcelain	Plastic	Glass	Paper	Mean
<b>AP</b>											
OpenMask3D (Takmaz et al. 2023)	19.1	12.7	28.0	26.5	9.1	0.1	41.8	16.9	23.1	10.7	18.8
SAI3D (Yin et al. 2024)	13.1	10.3	19.2	5.6	6.5	0.1	19.7	12.8	14.9	10.4	11.3
MaskClustering (Yan et al. 2024)	12.8	18.7	26.3	10.4	6.3	0.3	25.1	13.2	4.8	3.5	12.1
Open3DIS (Nguyen et al. 2024)	<b>32.9</b>	<b>27.1</b>	<b>35.4</b>	<b>33.0</b>	<b>24.6</b>	<b>2.4</b>	<b>43.1</b>	<b>33.8</b>	<b>29.9</b>	<b>20.9</b>	<b>28.3</b>
<b>AP<sub>50</sub></b>											
OpenMask3D (Takmaz et al. 2023)	23.9	16.0	30.4	30.3	11.6	0.1	44.5	20.0	29.7	15.2	22.1
SAI3D (Yin et al. 2024)	19.6	15.7	26.9	9.5	10.2	0.1	31.8	18.4	22.6	16.2	17.1
MaskClustering (Yan et al. 2024)	23.8	31.6	<b>41.0</b>	19.7	12.0	0.5	37.0	23.2	9.3	7.6	20.6
Open3DIS (Nguyen et al. 2024)	<b>40.9</b>	<b>32.7</b>	39.0	<b>38.6</b>	<b>30.7</b>	<b>3.5</b>	<b>46.3</b>	<b>38.8</b>	<b>37.6</b>	<b>27.8</b>	<b>33.6</b>
<b>AP<sub>25</sub></b>											
OpenMask3D (Takmaz et al. 2023)	27.4	19.1	32.5	33.5	13.3	0.1	47.0	21.7	34.8	21.4	25.0
SAI3D (Yin et al. 2024)	26.4	20.5	32.2	18.5	13.7	0.2	41.0	23.4	31.4	22.0	22.9
MaskClustering (Yan et al. 2024)	31.3	<b>38.4</b>	<b>49.7</b>	23.0	16.7	0.6	41.6	28.2	16.1	10.9	25.6
Open3DIS (Nguyen et al. 2024)	<b>44.7</b>	35.3	42.6	<b>42.2</b>	<b>33.5</b>	<b>5.1</b>	<b>48.3</b>	<b>42.4</b>	<b>41.8</b>	<b>31.6</b>	<b>36.7</b>

Table B: 3D instance segmentation results for the *material* aspect on our OpenScan benchmark.

Method	Affordance UpB X / ✓	Property UpB X / ✓	Type UpB X / ✓	Manner UpB X / ✓	Synonym UpB X / ✓	Requirement UpB X / ✓	Element UpB X / ✓	Mean UpB X / ✓
<b>AP</b>								
OpenMask3D	7.2 / 19.3 <sub>+12.1</sub>	7.5 / 26.7 <sub>+19.2</sub>	8.5 / 18.5 <sub>+10.0</sub>	12.8 / 27.7 <sub>+14.9</sub>	16.9 / 29.4 <sub>+12.5</sub>	13.0 / 26.5 <sub>+13.5</sub>	12.2 / 22.1 <sub>+9.9</sub>	9.7 / 21.6 <sub>+11.9</sub>
SAI3D	5.3 / 14.6 <sub>+9.3</sub>	5.8 / 17.7 <sub>+11.9</sub>	7.8 / 17.4 <sub>+9.6</sub>	11.3 / 18.9 <sub>+7.6</sub>	10.0 / 19.3 <sub>+9.3</sub>	10.0 / 19.2 <sub>+9.2</sub>	8.7 / 16.8 <sub>+8.1</sub>	7.6 / 16.8 <sub>+9.2</sub>
MaskClustering	6.2 / 15.4 <sub>+9.2</sub>	7.0 / 21.1 <sub>+14.1</sub>	7.1 / 13.9 <sub>+6.8</sub>	11.1 / 18.0 <sub>+6.9</sub>	16.2 / 18.0 <sub>+1.8</sub>	11.3 / 26.3 <sub>+15.0</sub>	7.4 / 17.6 <sub>+10.2</sub>	7.9 / 16.9 <sub>+9.0</sub>
Open3DIS	<b>11.9 / 23.9</b> <sub>+12.0</sub>	<b>12.8 / 36.0</b> <sub>+23.2</sub>	<b>14.2 / 24.5</b> <sub>+10.3</sub>	<b>19.2 / 34.9</b> <sub>+15.7</sub>	<b>26.7 / 36.1</b> <sub>+9.4</sub>	<b>19.2 / 35.0</b> <sub>+15.8</sub>	<b>18.7 / 28.0</b> <sub>+9.3</sub>	<b>15.4 / 27.7</b> <sub>+12.3</sub>
<b>AP<sub>50</sub></b>								
OpenMask3D	9.1 / 24.3 <sub>+15.2</sub>	10.0 / 34.2 <sub>+24.2</sub>	11.2 / 24.3 <sub>+13.1</sub>	15.4 / 35.1 <sub>+19.7</sub>	19.7 / 34.7 <sub>+15.0</sub>	16.0 / 34.4 <sub>+18.4</sub>	15.4 / 27.2 <sub>+11.8</sub>	12.2 / 27.4 <sub>+15.2</sub>
SAI3D	8.4 / 22.0 <sub>+13.6</sub>	8.3 / 27.7 <sub>+19.4</sub>	11.4 / 26.0 <sub>+14.6</sub>	15.7 / 28.4 <sub>+12.7</sub>	16.7 / 28.3 <sub>+11.6</sub>	15.3 / 30.1 <sub>+14.8</sub>	13.6 / 25.1 <sub>+11.5</sub>	11.5 / 25.4 <sub>+13.9</sub>
MaskClustering	10.7 / 28.6 <sub>+17.9</sub>	12.3 / 38.5 <sub>+26.2</sub>	13.3 / 26.8 <sub>+13.5</sub>	18.4 / 33.5 <sub>+15.1</sub>	30.3 / 34.2 <sub>+3.9</sub>	21.8 / <b>49.7</b> <sub>+27.9</sub>	13.5 / 32.5 <sub>+19.0</sub>	14.4 / 31.6 <sub>+17.2</sub>
Open3DIS	<b>14.8 / 29.9</b> <sub>+15.1</sub>	<b>16.0 / 43.8</b> <sub>+27.8</sub>	<b>17.9 / 30.6</b> <sub>+12.7</sub>	<b>22.3 / 43.1</b> <sub>+20.8</sub>	<b>30.6 / 42.6</b> <sub>+12.0</sub>	<b>24.1 / 43.8</b> <sub>+19.7</sub>	<b>21.9 / 33.5</b> <sub>11.6</sub>	<b>18.9 / 34.1</b> <sub>+15.2</sub>
<b>AP<sub>25</sub></b>								
OpenMask3D	10.4 / 27.6 <sub>+17.2</sub>	11.6 / 37.8 <sub>+26.2</sub>	13.0 / 27.4 <sub>+14.4</sub>	17.4 / 38.6 <sub>+21.2</sub>	20.6 / 37.4 <sub>+16.8</sub>	18.9 / 39.4 <sub>+20.5</sub>	17.1 / 31.2 <sub>+14.1</sub>	13.9 / 30.9 <sub>+17.0</sub>
SAI3D	10.5 / 28.3 <sub>+17.8</sub>	10.7 / 35.4 <sub>+24.7</sub>	13.4 / 33.2 <sub>+19.8</sub>	18.2 / 36.0 <sub>+17.8</sub>	20.0 / 32.9 <sub>+12.9</sub>	18.7 / 39.5 <sub>+20.8</sub>	16.0 / 32.4 <sub>+16.4</sub>	13.8 / 32.4 <sub>+18.6</sub>
MaskClustering	13.7 / <b>37.2</b> <sub>+23.5</sub>	15.8 / <b>48.8</b> <sub>+33.0</sub>	17.7 / <b>35.0</b> <sub>+17.3</sub>	23.1 / 44.8 <sub>+21.7</sub>	<b>36.6 / 45.0</b> <sub>+8.4</sub>	<b>28.2 / 61.6</b> <sub>+33.4</sub>	17.2 / <b>42.7</b> <sub>+25.5</sub>	18.5 / <b>41.0</b> <sub>+22.5</sub>
Open3DIS	<b>16.7 / 32.7</b> <sub>+16.0</sub>	<b>16.8 / 47.1</b> <sub>+30.3</sub>	<b>20.2 / 34.5</b> <sub>+14.3</sub>	<b>24.2 / 46.0</b> <sub>+21.8</sub>	33.1 / 44.9 <sub>+11.8</sub>	25.5 / 47.2 <sub>+21.7</sub>	<b>24.7 / 38.6</b> <sub>+13.9</sub>	<b>20.9 / 37.6</b> <sub>+16.7</sub>

Table C: 3D instance segmentation results with the upper bound on our OpenScan benchmark, where “UpB” denotes upper bound.

and Open3DIS (Nguyen et al. 2024) across 10 *material* attributes. It demonstrates that these OV-3D models perform strongly on the “porcelain” material, indicating that the visual information of the “porcelain” material in 3D objects (*e.g.*, “toilet” and “bathtub”) is more distinguishable than that of other materials. However, these OV-3D models struggle to accurately segment the “stone” material. This difficulty stems from the fact that stone is commonly associated with large 3D regions (*e.g.*, “wall” and “floor”), which are often neglected following the common practice (Schult et al. 2023; Takmaz et al. 2023; Yin et al. 2024) during 3D segmentation. These OV-3D models cannot correctly segment these large 3D areas, resulting in low results of the “stone” material. Notably, Open3DIS shows impressive results on each material compared to other OV-3D models, aligning with its strong performance in the classic OV-3D task.

#### C.4 Results of Upper Bound

During the 3D prediction in the GOV-3D task, we query the attributes to obtain the attribute-related 3D mask predictions. For annotating the OpenScan benchmark, object classes are associated with corresponding attributes using the ConceptNet (Speer, Chin, and Havasi 2017) database. Conversely, each attribute query can also be associated with the corresponding object classes. Therefore, we can replace the attribute queries with the ground truth attribute-related object classes from ConceptNet to finalize 3D mask results. We exclude the *material* aspect since the related object classes of *material* in the ConceptNet database are limited. We serve this setting as our upper bound performance. Table C shows the comparison of baseline methods OpenMask3D (Takmaz et al. 2023), SAI3D (Yin et al. 2024), MaskClustering (Yan et al. 2024), and Open3DIS (Nguyen et al. 2024) with their

Method	Affordance LLM X / ✓	Property LLM X / ✓	Type LLM X / ✓	Manner LLM X / ✓	Synonym LLM X / ✓	Requirement LLM X / ✓	Element LLM X / ✓	Material LLM X / ✓	Mean LLM X / ✓
<b>AP</b>									
OpenMask3D	7.2 / 10.8 <sub>+3.6</sub>	7.5 / 13.9 <sub>+6.4</sub>	8.5 / 8.5 <sub>+0</sub>	12.8 / 14.1 <sub>+1.3</sub>	16.9 / 25.7 <sub>+8.8</sub>	13.0 / 13.4 <sub>+0.4</sub>	12.2 / 12.1 <sub>-0.1</sub>	18.8 / 10.7 <sub>-8.1</sub>	9.9 / 11.7 <sub>+1.8</sub>
SAI3D	5.3 / 7.2 <sub>+1.9</sub>	5.8 / 9.9 <sub>+4.1</sub>	7.8 / 7.5 <sub>-0.3</sub>	11.3 / 14.5 <sub>+3.2</sub>	10.0 / 16.1 <sub>+6.1</sub>	10.0 / 9.3 <sub>-0.7</sub>	8.7 / 7.9 <sub>-0.8</sub>	11.3 / 6.6 <sub>-4.7</sub>	7.7 / 8.6 <sub>+0.9</sub>
MaskClustering	6.2 / 8.2 <sub>+2.0</sub>	7.0 / 8.5 <sub>+1.5</sub>	7.1 / 7.9 <sub>+0.8</sub>	11.1 / 9.1 <sub>-2.0</sub>	16.2 / 11.1 <sub>-5.1</sub>	11.3 / 16.1 <sub>+4.8</sub>	7.4 / 11.6 <sub>+4.2</sub>	12.1 / 8.9 <sub>-3.2</sub>	8.1 / 9.5 <sub>+1.4</sub>
Open3DIS	<b>11.9 / 15.1<sub>+3.2</sub></b>	<b>12.8 / 22.7<sub>+9.9</sub></b>	<b>14.2 / 15.4<sub>+1.2</sub></b>	<b>19.2 / 21.6<sub>+2.4</sub></b>	<b>26.7 / 31.0<sub>+4.3</sub></b>	<b>19.2 / 21.3<sub>+2.1</sub></b>	<b>18.7 / 17.6<sub>-1.1</sub></b>	<b>28.3 / 18.7<sub>-9.6</sub></b>	<b>15.8 / 17.8<sub>+2.0</sub></b>
<b>AP<sub>50</sub></b>									
OpenMask3D	9.1 / 13.5 <sub>+4.4</sub>	10.0 / 18.7 <sub>+8.7</sub>	11.2 / 11.0 <sub>-0.2</sub>	15.4 / 17.9 <sub>+2.5</sub>	19.7 / 30.7 <sub>+11.0</sub>	16.0 / 17.3 <sub>+1.3</sub>	15.4 / 15.0 <sub>-0.4</sub>	22.1 / 12.6 <sub>-9.5</sub>	12.5 / 14.7 <sub>+2.2</sub>
SAI3D	8.4 / 10.4 <sub>+2.0</sub>	8.3 / 15.7 <sub>+7.4</sub>	11.4 / 10.9 <sub>-0.5</sub>	15.7 / 20.7 <sub>+5.0</sub>	16.7 / 24.0 <sub>+7.3</sub>	15.3 / 15.1 <sub>-0.2</sub>	13.6 / 12.6 <sub>-1.0</sub>	17.1 / 10.0 <sub>-7.1</sub>	11.6 / 12.8 <sub>+1.2</sub>
MaskClustering	10.7 / 14.3 <sub>+3.6</sub>	12.3 / 16.3 <sub>+4.0</sub>	13.3 / 15.1 <sub>+1.8</sub>	18.4 / 16.1 <sub>-2.3</sub>	30.3 / 21.9 <sub>-8.4</sub>	21.8 / <b>30.5<sub>+8.7</sub></b>	13.5 / <b>21.2<sub>+7.7</sub></b>	20.6 / 15.7 <sub>-4.9</sub>	14.6 / 17.5 <sub>+2.9</sub>
Open3DIS	<b>14.8 / 18.7<sub>+3.9</sub></b>	<b>16.0 / 28.6<sub>+12.6</sub></b>	<b>17.9 / 18.8<sub>+0.9</sub></b>	<b>22.3 / 26.2<sub>+3.9</sub></b>	<b>30.6 / 36.9<sub>+6.3</sub></b>	<b>24.1 / 26.7<sub>+2.6</sub></b>	<b>21.9 / 21.0<sub>-0.9</sub></b>	<b>33.6 / 21.8<sub>-11.8</sub></b>	<b>19.3 / 21.7<sub>+2.4</sub></b>
<b>AP<sub>25</sub></b>									
OpenMask3D	10.4 / 15.3 <sub>+4.9</sub>	11.6 / 21.1 <sub>+9.5</sub>	13.0 / 14.3 <sub>+1.3</sub>	17.4 / 19.9 <sub>+2.5</sub>	20.6 / 33.2 <sub>+12.6</sub>	18.9 / 20.3 <sub>+1.4</sub>	17.1 / 17.0 <sub>-0.1</sub>	25.0 / 14.1 <sub>-10.9</sub>	14.2 / 17.1 <sub>+2.9</sub>
SAI3D	10.5 / 13.2 <sub>+2.7</sub>	10.7 / 20.2 <sub>+9.5</sub>	13.4 / 14.6 <sub>+1.2</sub>	18.2 / 23.3 <sub>+5.1</sub>	20.0 / 28.3 <sub>+8.3</sub>	18.7 / 18.9 <sub>+0.2</sub>	16.0 / 15.8 <sub>-0.2</sub>	22.9 / 13.4 <sub>-9.5</sub>	14.1 / 16.2 <sub>+2.1</sub>
MaskClustering	13.7 / 17.7 <sub>+4.0</sub>	15.8 / 20.4 <sub>+4.6</sub>	17.7 / 18.5 <sub>+0.8</sub>	23.1 / 22.4 <sub>-0.7</sub>	<b>36.6 / 26.7<sub>-9.9</sub></b>	<b>28.2 / 36.0<sub>+7.8</sub></b>	17.2 / <b>25.5<sub>+8.3</sub></b>	25.6 / 19.9 <sub>-5.7</sub>	18.7 / 21.5 <sub>+2.8</sub>
Open3DIS	<b>16.7 / 20.4<sub>+3.7</sub></b>	<b>16.8 / 30.2<sub>+13.4</sub></b>	<b>20.2 / 20.4<sub>+0.2</sub></b>	<b>24.2 / 28.2<sub>+4.0</sub></b>	33.1 / <b>39.2<sub>+6.1</sub></b>	25.5 / 28.5 <sub>+3.0</sub>	<b>24.7 / 23.4<sub>-1.3</sub></b>	<b>36.7 / 24.3<sub>-12.4</sub></b>	<b>21.4 / 23.6<sub>+2.2</sub></b>

Table D: 3D instance segmentation results with LLM for attribute understanding on our OpenScan benchmark.

upper bounds, highlighting significant performance gaps that underscore the potential for attribute-aware 3D reasoning.

## C.5 Results of Introducing LLM for Attribute Understanding

In our failure case analysis in the main paper, we observe that the OV-3D model Open3DIS (Nguyen et al. 2024) can identify the object classes (e.g., “piano”) in the OV-3D task but fails to recognize the associated object attributes (e.g., “this term has 88 keys”) in the GOV-3D task. This suggests a promising direction for improving GOV-3D performance by leveraging large language models (LLMs) to perform high-level reasoning, transforming the GOV-3D attribute queries (e.g., “this term has 88 keys”) back to the OV-3D class queries (e.g., “piano”). To this end, we design an experiment where an LLM (i.e., Vicuna-7B (Chiang et al. 2023)) is prompted to map object attributes to corresponding object classes. Given an attribute [attribute], the LLM is prompted as:

*Q: Given an object’s attribute [attribute], please output the related object’s classes in the indoor scene separated by commas.*

The LLM will generate a list of object classes corresponding to the input attribute [attribute]. We then format the object classes into a sentence as a query for evaluation. We utilize the baseline methods OpenMask3D (Takmaz et al. 2023), SAI3D (Yin et al. 2024), MaskClustering (Yan et al. 2024), and Open3DIS (Nguyen et al. 2024) to compare their performance on whether introducing LLM for attribute understanding. As shown in Table D, introducing LLM can improve the attribute understanding performance across most linguistic aspects of the GOV-3D task. However, performance declines in the *material* aspect, as LLMs rely exclusively on linguistic inputs and lack visual context required to differentiate material properties (e.g. “wooden chair” and “plastic chair”). Additionally, the LLM’s output can be noisy and inconsistent, occasionally producing object classes unrelated to the

Method	Mean			w-Mean		
	AP	AP <sub>50</sub>	AP <sub>25</sub>	AP	AP <sub>50</sub>	AP <sub>25</sub>
OpenMask3D	9.9	12.5	14.2	12.3	15.0	17.1
SAI3D	7.7	11.6	14.1	8.6	13.0	16.4
MaskClustering	8.1	14.6	18.7	9.0	16.0	20.3
Open3DIS	<b>15.8</b>	<b>19.3</b>	<b>21.4</b>	<b>19.1</b>	<b>23.1</b>	<b>25.5</b>

Table E: 3D instance segmentation results for weighted-mean score (w-Mean) on our OpenScan benchmark.

input attribute, which degrades performance in some linguist aspects.

## C.6 Results of Weighted Mean

In the OpenScan benchmark, we observe disparities in the attribute annotations for linguistic aspects (e.g., “affordance” and “synonym”). To address the imbalance in attribute annotations, we introduce a weighted mean score (w-Mean) metric that normalizes contributions based on annotation counts. For linguist aspects with annotation counts  $L = \{l_k\}_{k=1}^H$  and corresponding scores  $S = \{s_k\}_{k=1}^H$ , the w-Mean is computed as:

$$\text{w-Mean} = \frac{\sum_{k=1}^H s_k l_k}{\sum_{k=1}^H l_k} \quad (7)$$

As shown in Table E, applying the w-Mean metric improves the performance of baseline methods, including OpenMask3D (Takmaz et al. 2023), SAI3D (Yin et al. 2024), MaskClustering (Yan et al. 2024), and Open3DIS (Nguyen et al. 2024). This improvement steams from the w-Mean metric’s ability to normalize the contribution of each linguistic aspect based on its annotation count, thus mitigating biases from attributes and enhancing the robustness of performance evaluation across linguistic aspects in the GOV-3D task.

(a) Require complex commensense knowledge



**Class Query:**

*Plant*

**Attribute Query:**

*This term requires water and sun*

**Ground Truth**

**Image**

(b) Noisy 3D structure



**Class Query:**

*Paper towel dispenser*

**Attribute Query:**

*This term is used for dispensing toilet paper*

**Ground Truth**

**Image**

(c) Small object



**Class Query:**

*Cup*

**Attribute Query:**

*This term is used for drinking*

**Ground Truth**

**Image**

Figure C: Visualization of the Open3DIS failure cases. The ground truth objects and outputs are highlighted in color. Best view with zoom in.

## C.7 Additional Failure Cases Analysis

As illustrated in Figure C, the Open3DIS model(Nguyen et al. 2024) for OV-3D exhibits limitations in the GOV-3D task under specific conditions. Specifically, the model struggles to generate accurate 3D masks when: (a) the attribute query requires complex commonsense knowledge (e.g., “this term requires water and sun”), resulting in failure to predict 3D masks; (b) the target 3D object contains noisy geometry, such as 3D holes or irregular 3D structures, leading to partially incorrect 3D masks; and (c) the target object is small, providing insufficient geometric detail for segmentation, causing the model to fail in predicting 3D masks. In contrast, Open3DIS correctly predicts 3D masks for attribute-related class queries in the OV-3D task under these scenarios, underscoring the challenge of the GOV-3D task.

## D Additional Benchmark Details

### D.1 Does OpenScan Represent 200 Object Classes From ScanNet200 Well Enough?

During the annotation of our OpenScan benchmark, object classes from ScanNet200 (Rozenberszki et al. 2022) are labeled with attributes using the ConceptNet (Speer, Chin, and Havasi 2017) database and manual annotation. Figure D shows the number of attributes per object class from ScanNet200 in our OpenScan benchmark. Notably, most object classes from ScanNet200 are annotated with more than one attribute in our OpenScan, indicating that our OpenScan benchmark adequately represents object classes from ScanNet200. Besides, the object class has up to seven attributes (i.e., “bicycle”, and “ball”) in our OpenScan benchmark.

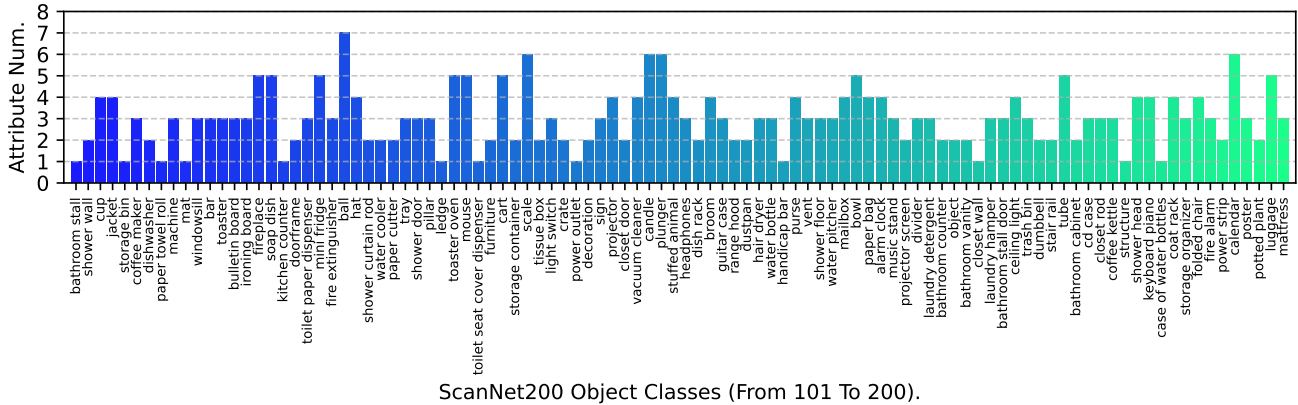
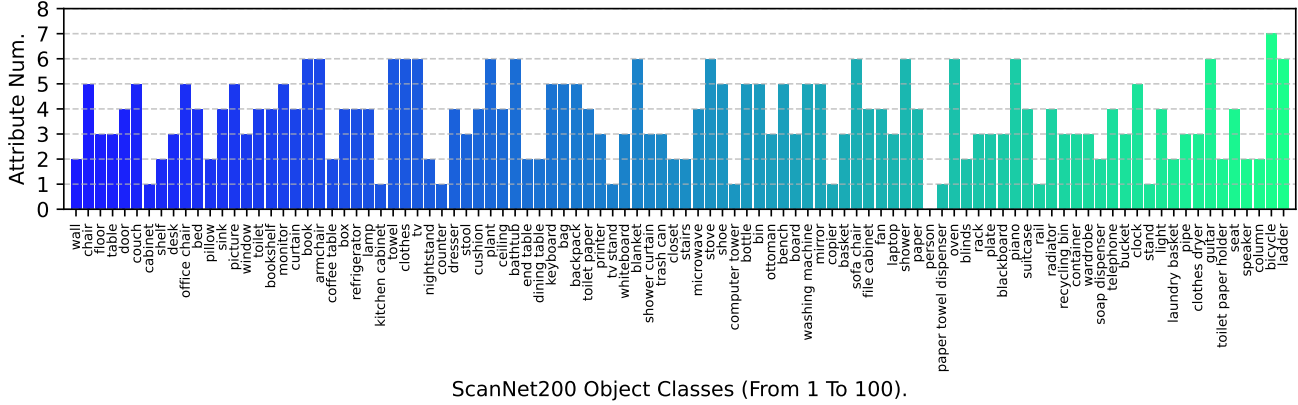


Figure D: Number of attributes per object class from ScanNet200 in our OpenScan benchmark.

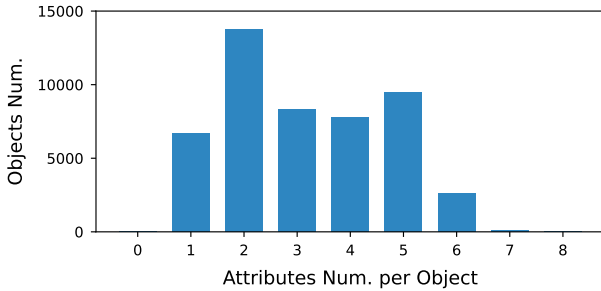


Figure E: Number of attributes per object in our OpenScan benchmark and corresponding number of objects.

## D.2 Number of Attributes per Object.

Figure E summarizes the distribution of attributes per object in our OpenScan benchmark. The majority of objects have 1–6 attributes.

## D.3 Number of Attributes per Scene.

Figure F presents the distribution of attributes per scene in our OpenScan benchmark. It demonstrates that the attributes in 3D scenes are semantically rich.

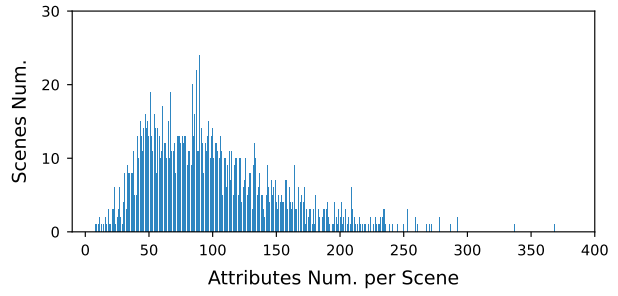


Figure F: Number of attributes per scene in our OpenScan benchmark and corresponding number of scenes.

## D.4 Attribute Verification in Benchmark Annotation

During the attribute annotation process, we leverage a knowledge graph to automatically generate object-related attributes. However, the initial attribute set often contains noise, including attributes that are irrelevant, ambiguous, or semantically inconsistent with the related object classes. To address this, we conduct a meticulous manual verification process to refine the attribute set, ensuring semantic consistency and coherence in our OpenScan benchmark.

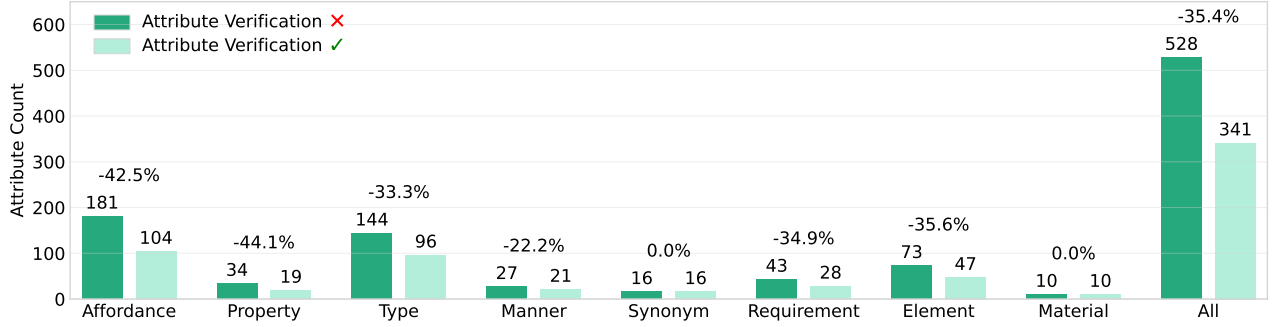


Figure G: OpenScan benchmark statistics of attributes during attribute verification.

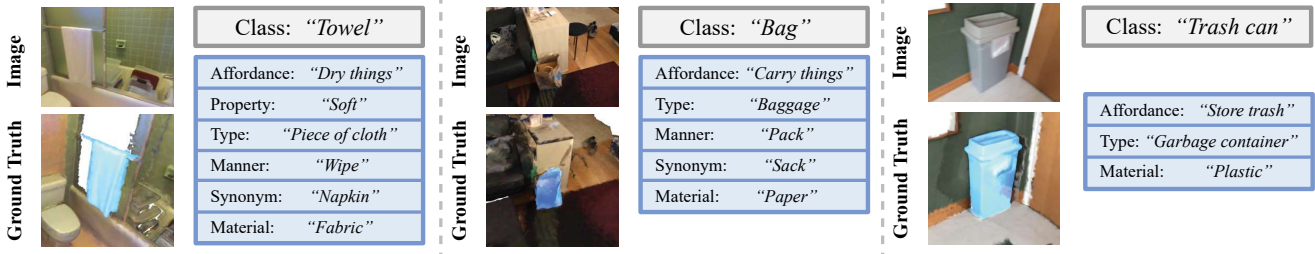


Figure H: Examples of objects and corresponding attributes in our OpenScan benchmark.

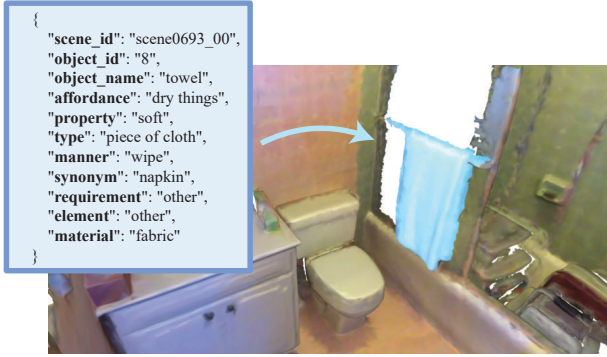


Figure I: OpenScan benchmark format. The target object is highlighted in blue.

As shown in Figure G, our OpenScan benchmark generates 528 attributes initially. After attribute verification, 341 attributes are retained, resulting in an overall reduction of 35.4% of noisy attributes. Notably, the *affordance* aspect exhibits high noise level, with 42.5% of attributes being filtered out, suggesting that the *affordance* attributes are particularly prone to ambiguity due to the diverse nature of affordance candidates within the knowledge graph. In contrast, all *synonym* attributes are retained during verification. This robustness is attributed to the high semantic similarity between synonym attributes and their corresponding object classes, ensuring reliable alignment during the generation process.

## D.5 Additional Benchmark Samples

We provide additional samples of our OpenScan benchmark. Figure H presents the examples of objects and their corresponding attributes. Figure J displays the *affordance*, *property*, *type*, and *manner* aspects, while Figure K shows the *synonym*, *requirement*, *element*, and *material* aspects.

## D.6 Benchmark Formats

Figure I shows an example of our OpenScan benchmark formats. Our OpenScan is formatted in the JSON file. Each target 3D object is annotated with the following items:

- **Scene ID:** indicates the scene in which the target object is located.
- **Object ID:** identifies the target object's unique ID within the scene.
- **Object Name:** specifies the object class of the target object.

In addition, each object is annotated with eight linguistic aspects (*affordance*, *property*, *type*, *manner*, *synonym*, *requirement*, *element*, and *material*). If the target 3D object does not contain an attribute of a specific linguistic aspect, it is marked as “other”.

## D.7 Benchmark Details

We construct our OpenScan benchmark based on ScanNet200 (Rozenberszki et al. 2022) across eight linguistic aspects. We present all attributes and their corresponding

query templates in our OpenScan benchmark: Table F displays the *affordance* and *property* aspects; Table G shows the *type*, *manner*, and *synonym* aspects; and Table H presents the *requirement*, *element*, and *material* aspects. The “object” in the query template is replaced with “this term” in our experiments.

## E Additional Related Work

**Open-Vocabulary 2D Understanding Benchmarks.** Open-vocabulary 2D understanding refers to the task of detecting or segmenting novel object classes that are not present in the training dataset. For the object detection task, COCO (Lin et al. 2014) and LVIS (Gupta, Dollar, and Girshick 2019) are two widely used datasets. For the image segmentation task, popular datasets include COCO (Lin et al. 2014), ADE20k (Zhou et al. 2019), PASCAL-VOC (Everingham et al. 2015), and Cityscapes (Cordts et al. 2016). However, these benchmarks primarily evaluate the model’s open-vocabulary ability but do not explicitly assess its capability to recognize specific object characteristics. PACO (Ramanathan et al. 2023) introduces a 2D segmentation benchmark that focuses on parts and attributes of common objects. Inspired by PACO (Ramanathan et al. 2023), FG-OVD (Bianchi et al. 2024) presents a challenging task and benchmark for fine-grained open-vocabulary object detection to evaluate the ability of open-vocabulary detectors to discern extrinsic object properties. Similarly, OVDEval (Yao et al. 2024) introduces an open-vocabulary detection benchmark to evaluate the performance on linguistic aspects using complex language prompts. Our work is different from them (Ramanathan et al. 2023; Bianchi et al. 2024; Yao et al. 2024) since we focus on the understanding of object attributes on 3D data, which poses greater challenges compared to the understanding in 2D images due to the limited annotations in 3D benchmarks.

## F Limitations and Future Work

Our benchmark is currently constructed solely on the ScanNet200 benchmark with limited 3D indoor scene. It would be beneficial to increase the scale of our benchmark to include a wider variety of 3D scenes and objects. In future work, we plan to extend our OpenScan benchmark to encompass more diverse scenes by incorporating indoor 3D datasets such as ScanNet++ (Yeshwanth et al. 2023) and Matterport3D (Chang et al. 2017). Our mature annotation procedures can be readily adapted to these datasets. Moreover, we aim to evaluate current OV-3D models on our GOV-3D task, particularly examining performance variations when using higher point resolutions in ScanNet++ (Yeshwanth et al. 2023) and larger scene areas in Matterport3D (Chang et al. 2017).

## G Broader Impact

Our approach does not introduce any negative societal impacts. All experiments are performed on publicly available datasets, with no use of private data. Although our benchmark is constructed exclusively from public data, we recognize the potential for unintended consequences if the data is applied without appropriate safeguards. We urge readers to

ensure that the application of this research remains lawful and ethical, strictly adhering to established regulations and guidelines.

Query	Affordance	Property	Type	Manner
Image	<i>This term is used for climbing walls</i>	<i>This term is bright</i>	<i>This term is a garbage container</i>	<i>This term can be worn on head</i>
Ground Truth				
Image				
Query	<i>This term is used for putting out fires</i>	<i>This term is round</i>	<i>This term is a piece of cloth</i>	<i>This term is a way of quantifying</i>
Image				
Ground Truth				
Query	<i>This term is used for drying your hair</i>	<i>This term is soft</i>	<i>This term is an organism</i>	<i>This term can be played</i>
Image				
Ground Truth				

Figure J: Additional OpenScan benchmark samples of *affordance*, *property*, *type*, and *manner* aspects. Target objects are highlighted in blue.

	Synonym	Requirement	Element	Material
Query	<i>This term is similar to image</i>	<i>Making a phone call requires this term</i>	<i>This term has two wheels</i>	<i>This term is made of wood</i>
Ground Truth				
Query	<i>This term is related to sack</i>	<i>Cleaning your room requires this term</i>	<i>This term has blades</i>	<i>This term is made of porcelain</i>
Ground Truth				
Query	<i>This term is related to ornament</i>	<i>Cooking a curry requires this term</i>	<i>This term has six strings</i>	<i>This term is made of metal</i>
Ground Truth				
Image				

Figure K: Additional OpenScan benchmark samples of *synonym*, *requirement*, *element*, and *material* aspects. Target objects are highlighted in blue.

	Attribute	Template	Attribute	Template
Affordance	carry things rest keep food cold work bath stand measure weight display images poop bake toaster making toast separate rooms ride see yourself dry things storage dirty clothes represent heat the room presenting information cool a person heat a room protecting your head store liquids transport things communicate carrying money learning carry liquids write ideas and terms on make a captured voice become audible eat dinner furnish have privacy blow your nose bounce organize books climb drink hold sheet music hang clothes control a computer keep clothes climb walls hold things putting out fires hang coat hold food show movies wash clothes vacumming decorating your room receiving letters	[object] is used for carrying things [object] is used for resting [object] is used for keeping food cold [object] is used for working [object] is used for bathing [object] is used for standing [object] is used for measuring weight [object] is used for displaying images [object] is used for pooping [object] is used for baking toaster [object] is used for making toast [object] is used for separating rooms [object] is used for riding [object] is used for seeing yourself [object] is used for drying things [object] is used for storing dirty clothes [object] is used for representing [object] is used for heating the room [object] is used for presenting information [object] is used for cooling a person [object] is used for heating a room [object] is used for protecting your head [object] is used for storing liquids [object] is used for transporting things [object] is used for communicating [object] is used for carrying money [object] is used for learning [object] is used for carrying liquids [object] is used for writing ideas and terms on [object] is used for making a captured voice become audible [object] is used for eating dinner [object] is used for furnishing [object] is used for having privacy [object] is used for blowing your nose [object] is used for bouncing [object] is used for organizing books [object] is used for climbing [object] is used for drinking [object] is used for holding sheet music [object] is used for hanging clothes [object] is used for controlling a computer [object] is used for keeping clothes [object] is used for climbing walls [object] is used for holding things [object] is used for putting out fires [object] is used for hanging coat [object] is used for holding food [object] is used for showing movies [object] is used for washing clothes [object] is used for vacumming [object] is used for decorating your room [object] is used for receiving letters	holding up a roof sit place coffee look outside cover a window wash dishes store trash sleep tell time perform music heat food close the top of a room store books store guitar put your feet on hold up the roof hang clothes make coffee grow in a garden foot protection illuminate an area print documents keep out light from houses collect recyclable plastics pack clothes for a trip wear store things turn on a light store file type bake cookies detect fire hold toilet paper store water cover a bed hold trash store clothes listen to music unlocking a toilet entertain a child dispense toilet paper entry and exit to the shower hold soap get drunk carry something spray water dry your hair dry clothes mark that special date ironing clothes sweeping hold cd	[object] is used for holding up a roof [object] is used for sitting [object] is used for placing coffee [object] is used for looking outside [object] is used for covering a window [object] is used for washing dishes [object] is used for storing trash [object] is used for sleeping [object] is used for telling time [object] is used for performing music [object] is used for heating food [object] is used for closing the top of a room [object] is used for storing books [object] is used for storing guitar [object] is used for putting your feet on [object] is used for holding up the roof [object] is used for hanging clothes [object] is used for making coffee [object] is used for growing in a garden [object] is used for foot protection [object] is used for illuminating an area [object] is used for printing documents [object] is used for keeping out light from houses [object] is used for collecting recyclable plastics [object] is used for packing clothes for a trip [object] is used for wearing [object] is used for storing things [object] is used for turning on a light [object] is used for storing file [object] is used for typing [object] is used for baking cookies [object] is used for detecting fire [object] is used for holding toilet paper [object] is used for storing water [object] is used for covering a bed [object] is used for holding trash [object] is used for storing clothes [object] is used for listening to music [object] is used for unblocking a toilet [object] is used for entertaining a child [object] is used for dispensing toilet paper [object] is used for entry and exit to the shower [object] is used for holding soap [object] is used for getting drunk [object] is used for carrying something [object] is used for spraying water [object] is used for drying your hair [object] is used for drying clothes [object] is used for marking that special date [object] is used for ironing clothes [object] is used for sweeping [object] is used for holding cd
Property	useful for camping opaque and closed helpful in making comparisons hot open or closed fun to ride alive hollow useful for unblocking a toilet convex down	[object] is useful for camping [object] is opaque and closed [object] is helpful in making comparisons [object] is hot [object] is open or closed [object] is fun to ride [object] is alive [object] is hollow [object] is useful for unblocking a toilet [object] is convex down	soft essential for privacy analog or digital one kind of stringed instrument horizontal reflective bright round shaped like a shell	[object] is soft [object] is essential for privacy [object] is analog or digital [object] is one kind of stringed instrument [object] is horizontal [object] is reflective [object] is bright [object] is round [object] is shaped like a shell

Table F: OpenScan benchmark attributes of *affordance* and *property* aspects.

	<b>Attribute</b>	<b>Template</b>	<b>Attribute</b>	<b>Template</b>
Type	baggage table were someone works window covering measuring instrument a way to relax vanity basket string instrument appliances upper surface reflector piece of cloth clue a cooling device heater a form of clothing dispenser a vehicle a communication device coat tube sill board portable computer computer device alarm paper an instrument of music bedclothes shelf supporter trophy vessel rod bag a container for clothes stairs firefighting equipment device for spraying clock hood optical device detergent screen pad electronic piano household cleaning tool receptacle container	[object] is a baggage [object] is a table were someone works [object] is a window covering [object] is a measuring instrument [object] is a way to relax [object] is a vanity [object] is a basket [object] is a string instrument [object] is an appliance [object] is an upper surface [object] is a reflector [object] is a piece of cloth [object] is a clue [object] is a cooling device [object] is a heater [object] is a form of clothing [object] is a dispenser [object] is a vehicle [object] is a communication device [object] is a coat [object] is a tube [object] is a sill [object] is a board [object] is a portable computer [object] is a computer device [object] is an alarm [object] is a paper [object] is an instrument of music [object] is a bedclothes [object] is a shelf [object] is a supporter [object] is a trophy [object] is a vessel [object] is a rod [object] is a bag [object] is a container for clothes [object] is stairs [object] is a firefighting equipment [object] is a device for spraying [object] is a clock [object] is a hood [object] is an optical device [object] is a detergent [object] is a screen [object] is a pad [object] is an electronic piano [object] is a household cleaning tool [object] is a receptacle container	seat plumbing fixture land garbage container a good place to lie kitchen appliance box rack movable barrier a two wheel vehicle container representation organism footwear source of illumination refrigerator a long seat with no backrest bin handbag an excellent source of information switch door cabinet display shaft curtain bottle a toy cutting implement table railing audio device a tool to unclog toilets padding toy animal hole storage device fitness equipment counter kettle beauty device dryer machine drafting instrument pitcher time list sign a container for letters	[object] is a seat [object] is a plumbing fixture [object] is a land [object] is a garbage container [object] is a good place to lie [object] is a kitchen appliance [object] is a box [object] is a rack [object] is a movable barrier [object] is a two wheel vehicle [object] is a container [object] is a representation [object] is an organism [object] is a footwear [object] is a source of illumination [object] is a refrigerator [object] is a long seat with no backrest [object] is a bin [object] is a handbag [object] is an excellent source of information [object] is a switch [object] is a door [object] is a cabinet [object] is a display [object] is a shaft [object] is a curtain [object] is a bottle [object] is a toy [object] is a cutting implement [object] is a table [object] is a railing [object] is an audio device [object] is a tool to unclog toilets [object] is a padding [object] is a toy animal [object] is a hole [object] is a storage device [object] is a fitness equipment [object] is a counter [object] is a kettle [object] is a beauty device [object] is a dryer [object] is a machine [object] is a drafting instrument [object] is a pitcher [object] is a time list [object] is a sign [object] is a container for letters
Manner	pack bathe cook wipe worn on a head written on played with used in a toilet climbed to reach some place high produce schedule	[object] is a way of packing [object] is a way of bathing [object] is a way of cooking [object] is a way of wiping [object] can be worn on a head [object] can be written on [object] can be played with [object] can be used in a toilet [object] can be climbed to reach some place high [object] is a way of producing [object] is a way of scheduling	observe quantify steered by handlebars wear transport things played cover bed manipulate computer store lit with a match	[object] is a way of observing [object] is a way of quantifying [object] can be steered by handlebars [object] is a way of wearing [object] is a way of transporting things [object] can be played [object] is a way of covering bed [object] is a way of manipulating computer [object] is a way of storing [object] can be lit with a match
Synonym	weight bedside table image reading power bar ornament dress suitcase	[object] is related to weight [object] is related to bedside table [object] is similar to image [object] is related to reading [object] is related to power bar [object] is related to ornament [object] is related to dress [object] is related to suitcase	news napkin sack pipe round suction cup houseplant almanac	[object] is related to news [object] is related to napkin [object] is related to sack [object] is related to pipe [object] is related to round [object] is similar to suction cup [object] is related to houseplant [object] is related to almanac

Table G: OpenScan benchmark attributes of *type*, *manner*, and *synonym* aspects.

	<b>Attribute</b>	<b>Template</b>	<b>Attribute</b>	<b>Template</b>
<b>Requirement</b>	sit down	sitting down requires [object]	be unplugged	[object] does not desire to be unplugged
	have a bath	having a bath requires [object]	using a VCR	using a VCR requires [object]
	wake up in the morning	waking up in the morning requires [object]	playing a guitar	playing a guitar requires [object]
	balance to ride	[object] requires balance to ride	grooming	grooming requires [object]
	get warm	getting warm requires [object]	water and sun	[object] requires water and sun
	print	printing requires [object]	drink	drinking requires [object]
	buying food	buying food requires [object]	make a phone call	making a phone call requires [object]
	bring suit	bringing suit requires [object]	go on the internet	going on the internet requires [object]
	write	writing requires [object]	type	typing requires [object]
	cook a curry	cooking a curry requires [object]	play the piano	playing the piano requires [object]
	playing soccer	playing soccer requires [object]	eating breakfast in bed	eating breakfast in bed requires [object]
	paint a house	painting a house requires [object]	going on a vacation	going on a vacation requires [object]
	a goldfish	a goldfish requires [object]	washing your clothes	washing your clothes requires [object]
	cleaning clothing	cleaning clothing requires [object]	cleaning your room	cleaning your room requires [object]
<b>Element</b>	water	[object] has water	news	[object] has news
	urine	[object] has urine	twelve numbers	[object] has twelve numbers
	toaster	[object] has toaster	six strings	[object] has six strings
	two wheels	[object] has two wheels	doorway	doorway has [object]
	legs	[object] has legs	an art show	an art show has [object]
	fire	[object] has fire	ecosystem	ecosystem has [object]
	blades	[object] has blades	foot	[object] has foot
	heating system	heating system has [object]	money	[object] has money
	knowledge	[object] has knowledge	six sides	[object] has six sides
	circuit	circuit has [object]	window frame	window frame has [object]
	bathroom	bathroom has [object]	a document folder	[object] has a document folder
	screen	[object] has screen	keys	[object] has keys
	food	[object] has food	88 keys	[object] has 88 keys
	books	[object] has books	trash	[object] has trash
	tack	[object] has tack	clothes	[object] has clothes
	sofa	sofa has [object]	computer	computer has [object]
	toilet paper	[object] has toilet paper	air passage	air passage has [object]
	rundle	rundle has [object]	soap	[object] has soap
	beer	[object] has beer	a coat	[object] has a coat
<b>Material</b>	a shower stall	a shower stall has [object]	table	table has [object]
	the movies	the movies have [object]	clothing	[object] has clothing
	bed	bed has [object]	a wick	[object] has a wick
	the date	[object] has the date	mail	[object] has mail
	a cd	[object] has a cd		
	wood	[object] is made of wood	fabric	[object] is made of fabric
	leather	[object] is made of leather	cotton	[object] is made of cotton
	metal	[object] is made of metal	stone	[object] is made of stone
	porcelain	[object] is made of porcelain	plastic	[object] is made of plastic
	glass	[object] is made of glass	paper	[object] is made of paper

Table H: OpenScan benchmark attributes of *requirement*, *element*, and *material* aspects.